AGU PUBLICATIONS

JGR

Journal of Geophysical Research: Atmospheres

RESEARCH ARTICLE

10.1002/2015JD024297

Special Section:
Studies of Emissions and Atmospheric Composition, Clouds and Climate Coupling by Regional Surveys, 2013 (SEAC4RS)

Key Points:
- The SEAC4RS field mission was based near Houston, Texas during August and September of 2013
- The paper overviews the mission to aid those interested in this data set to understand its context
- The data can be accessed at http://www-air.larc.nasa.gov/cgi-bin/ArcView/seac4rs

Correspondence to:
O. B. Toon,
toon@lasp.colorado.edu

Citation:
Toon, O. B., et al. (2016), Planning, implementation, and scientific goals of the Studies of Emissions and Atmospheric Composition, Clouds and Climate Coupling by Regional Surveys (SEAC^{4}RS) field mission, *J. Geophys. Res. Atmos.*, *121*, 4967–5009, doi:10.1002/2015JD024297.

Received 30 SEP 2015
Accepted 30 MAR 2016
Accepted article online 5 APR 2016
Published online 4 May 2016

Planning, implementation, and scientific goals of the Studies of Emissions and Atmospheric Composition, Clouds and Climate Coupling by Regional Surveys (SEAC^{4}RS) field mission

Owen B. Toon[1], Hal Maring[2], Jack Dibb[3], Richard Ferrare[4], Daniel J. Jacob[5], Eric J. Jensen[6], Z. Johnny Luo[7], Gerald G. Mace[8], Laura L. Pan[9], Lenny Pfister[6], Karen H. Rosenlof[10], Jens Redemann[6], Jeffrey S. Reid[11], Hanwant B. Singh[6], Anne M. Thompson[12], Robert Yokelson[13], Patrick Minnis[4], Gao Chen[4], Kenneth W. Jucks[2], and Alex Pszenny[2]

[1]Department of Atmospheric and Oceanic Sciences and Laboratory for Atmospheric and Space Physics, University of Colorado Boulder, Boulder, Colorado, USA, [2]NASA Headquarters, Washington, District of Columbia, USA, [3]Department of Earth Sciences and Institute for the Study of Earth, Oceans, and Space, University of New Hampshire, Durham, New Hampshire, USA, [4]NASA Langley Research Center, Hampton, Virginia, USA, [5]School of Engineering and Applied Sciences, Harvard University, Cambridge, Massachusetts, USA, [6]NASA Ames Research Center, Moffett Field, California, USA, [7]Department of Earth and Atmospheric Sciences and Cooperative Remote Sensing Science and Technology Center, City College of New York, New York, New York, USA, [8]Department of Atmospheric Sciences, University of Utah, Salt Lake City, Utah, USA, [9]National Center for Atmospheric Research, Boulder, Colorado, USA, [10]NOAA Earth System Research Laboratory, Boulder, Colorado, USA, [11]Naval Research Laboratory, Monterey, California, USA, [12]NASA Goddard Space Flight Center, Greenbelt, Maryland, USA, [13]Department of Chemistry, University of Montana, Missoula, Montana, USA

Abstract The Studies of Emissions and Atmospheric Composition, Clouds and Climate Coupling by Regional Surveys (SEAC^{4}RS) field mission based at Ellington Field, Texas, during August and September 2013 employed the most comprehensive airborne payload to date to investigate atmospheric composition over North America. The NASA ER-2, DC-8, and SPEC Inc. Learjet flew 57 science flights from the surface to 20 km. The ER-2 employed seven remote sensing instruments as a satellite surrogate and eight in situ instruments. The DC-8 employed 23 in situ and five remote sensing instruments for radiation, chemistry, and microphysics. The Learjet used 11 instruments to explore cloud microphysics. SEAC^{4}RS launched numerous balloons, augmented AErosol RObotic NETwork, and collaborated with many existing ground measurement sites. Flights investigating convection included close coordination of all three aircraft. Coordinated DC-8 and ER-2 flights investigated the optical properties of aerosols, the influence of aerosols on clouds, and the performance of new instruments for satellite measurements of clouds and aerosols. ER-2 sorties sampled stratospheric injections of water vapor and other chemicals by local and distant convection. DC-8 flights studied seasonally evolving chemistry in the Southeastern U.S., atmospheric chemistry with lower emissions of NO_x and SO_2 than in previous decades, isoprene chemistry under high and low NO_x conditions at different locations, organic aerosols, air pollution near Houston and in petroleum fields, smoke from wildfires in western forests and from agricultural fires in the Mississippi Valley, and the ways in which the chemistry in the boundary layer and the upper troposphere were influenced by vertical transport in convective clouds.

1. Introduction

The Studies of Emissions and Atmospheric Composition, Clouds and Climate Coupling by Regional Surveys (SEAC^{4}RS) field mission was based at Ellington Field, near Houston, Texas, in August and September 2013. The more than 450 participants came from multiple National Aeronautics and Space Administration centers, the Naval Research Laboratory, National Oceanographic and Atmospheric Agency laboratories, the National Center for Atmospheric Research, numerous universities, and private research institutions in the United States. The NASA ER-2, the NASA DC-8, and the SPEC Inc. Learjet flew a total of 57 science flights during SEAC^{4}RS. SEAC^{4}RS employed the most comprehensive airborne payload to date to investigate atmospheric composition over North America. The SEAC^{4}RS mission was sponsored by three program offices at NASA, as well as the Naval Research Laboratory, and consequently had a broad set of goals designed to understand issues related to the lower stratosphere, the Earth's radiation budget, and tropospheric chemistry. One unifying goal was to understand how radiatively and chemically important atmospheric constituents are transported vertically through the atmospheric column from the ground to the lower stratosphere. SEAC^{4}RS

was closely related to the 2012 Deep Convective Clouds and Chemistry Experiment (DC3), sponsored by the U.S. National Science Foundation and NASA, which shared this unifying goal and used the NASA DC-8 with a very similar payload to the one used in SEAC^{4}RS [*Barth et al.*, 2014].

SEAC^{4}RS was initially planned to take place in Southeast Asia in the summer of 2012. However, political barriers made it impossible to operate in the region. Consequently, SEAC^{4}RS was repositioned to the U.S. in the summer of 2013 where many of our goals were achieved.

Due to its complexity and broad range of goals the SEAC^{4}RS mission was planned and executed by a large group of scientists with expertise in a variety of fields. The mission was an enriching and enlightening experience due to the many points of view, many research goals, and great range of scientific expertise that were involved. Generally, plans for each flight were designed by several groups with differing goals and then debated in an open forum. The plan with the greatest chance of success and priority was then chosen subject to the evolving weather, instrument status, and the presence of unique opportunities (such as large wild fires) or fleeting opportunities due to temperature sensitivity of targeted chemical emissions and seasonal variability. The SEAC^{4}RS science team is listed under "Participants" on the NASA Earth Science project office website (https://espo.nasa.gov/home/seac4rs/content/SEAC4RS). This list indicates the various science areas involved, as well as some of the modeling tools used in flight planning. The reader may contact individual science team members for detailed questions about the mission and about data analysis.

SEAC^{4}RS interacted with a number of other field programs. The Department of Energy's Biomass Burning Observation Project (BBOP) took place in the Pacific Northwest during July–August 2013 and in the Mississippi Valley during October 2013. On one occasion, 6 August, the SEAC^{4}RS aircraft and the BBOP aircraft sampled plumes from the same complex of fires in Southwest Oregon. NASA's DISCOVER-AQ program made flights from Ellington Field in Houston, Texas, during September 2013. SEAC^{4}RS made a number of measurements related to the goals of DISCOVER-AQ to better understand urban air pollution in the Houston area and how to use satellite measurements to measure air quality. SEAC^{4}RS immediately followed, and in many ways extended, the NSF, NOAA, EPA, EPRI Southeast Atmosphere Study (SAS) carried out during June and July 2013. SAS was an umbrella program for several related programs, the Southern Oxidant and Aerosol Study (SOAS), the North American Airborne Mercury Experiment (NAAMEX), the Tropospheric HONO project (TROPHONO), the Nitrogen, Oxidants, and Aerosol Distributions, Sources and Sinks (NOMADSS) project and Southeast Nexus study (SENEX) all aimed at airborne and ground-based measurements of air chemistry in the Southeastern United States.

This paper provides context and an overview of the SEAC^{4}RS mission for those interested in using this data set for their scientific studies. The SEAC^{4}RS data are now in the public domain and can be accessed at http://www-air.larc.nasa.gov/cgi-bin/ArcView/seac4rs. Alternatively, one can locate the data at www.doi.org using doi:10.5067/Aircraft/SEAC4RS/Aerosol-TraceGas-Cloud. Section 2 describes the goals for SEAC^{4}RS, and discusses the scientific motivations for the goals. Section 3 discusses the meteorological context for the mission and compares with climatology from previous years. Section 4 discusses the instrument packages on the aircraft and the other platforms, and also summarizes the various flights that were conducted and how these flights relate to the goals of the mission. Section 5 concludes by summarizing briefly the findings of the papers that have been published to date.

2. Scientific Motivation and Key Questions

Table 1 lists the major goals that SEAC^{4}RS sought to address. These goals cover a broad range of atmospheric science, reflecting the three NASA programs that supported SEAC^{4}RS: Radiation Sciences, Tropospheric Chemistry, and Upper Atmosphere Research.

Table 2 lists a series of specific questions used to design flight plans. Table 3 provides a calendar of the flights conducted in SEAC^{4}RS and relates the goals of the flights to the questions in Table 2. This approach of tracking the connection between flights and the questions they addressed was used to measure the progress that was made in addressing the questions during the mission. The science rationale for the questions in Table 2 is discussed below.

Table 1. Major Goals of SEAC^{4}RS

	Goal
1.	To determine how pollutant emissions are redistributed via deep convection throughout the troposphere.
2.	To determine the evolution of gases and aerosols in deep convective outflow and the implications for chemistry in the upper troposphere and lower stratosphere.
3.	To identify the influences and feedbacks of aerosol particles from anthropogenic pollution and biomass burning on meteorology and climate through changes in the atmospheric heat budget or through microphysical changes in clouds.
4.	To understand how anthropogenic and biogenic emissions interact to control tropospheric ozone and aerosol concentrations.
5.	To serve as a calibration/validation test bed for future satellite instruments and missions.

2.1. Upper Atmosphere Research

As noted in Table 2, SEAC^{4}RS had three basic goals related to the upper troposphere and lower stratosphere (UTLS). These goals are primarily related to transport of tracers and water vapor into the lower stratosphere during the North American Monsoon (NAM) season and to determining the structure of the lower stratosphere during the late summer.

2.1.1. Do Individual Deep Convective Cloud Systems Locally Inject Water Vapor and Other Chemicals Into the Overworld Stratosphere Over the U.S.?

Water vapor in the tropopause region plays a significant role in the radiative forcing of the surface climate [*Solomon et al.*, 2010]. Deep convection may serve as a transport pathway for injecting water vapor and other tropospheric source constituents into the stratosphere, including as high as the overworld, which is that part of the stratosphere above the tropical tropopause height (~380 K potential temperature). *Schwartz et al.* [2013] show from Microwave Limb Sounder data that the midlatitude lowermost stratosphere often has significant enhancements of water vapor during the summer months. *Homeyer et al.* [2014] found from the NASA DC-8 and the NSF Gulf-Stream V in the May–June 2012 DC3 mission that significant water vapor perturbations in the UTLS occurred above mesoscale complexes, individual convective cells, and a convective line, particularly when a double tropopause was present. *Hanisco et al.* [2007] and *Anderson et al.* [2012] used in situ

Table 2. Specific Questions Used to Define Flight Plans

Atmospheric Science Area	Question
Upper atmosphere research	1. Do deep convective cloud systems locally inject water vapor and other chemicals into the overworld stratosphere over the U.S.?
	2. What role does the North American Monsoon play in transporting water vapor and pollutants into the lower stratosphere?
	3. What are the water and tracer distributions in the stratosphere?
Tropospheric chemistry	1. How has the chemistry changed over the Southeastern U.S. as pollution from NO_x, and SO_2 declined?
	2. Can isoprene levels be inferred from satellite measurements of formaldehyde?
	3. How does the seasonal transition from summer to fall impact atmospheric chemistry in the U.S. southeast?
	4. Is the air chemistry significantly modified over regions with large oilfields and fracking?
	5. What are the properties and transformations of organic gases and aerosols in the Southeastern U.S.?
	6. How do the properties of smoke vary between wildfires in the Western U.S. and agricultural fires in the Mississippi Valley?
	7. How does vertical transport modify the chemistry of the upper troposphere?
	8. What are the air quality impacts of urban areas, power plants, and other localized sources?
Radiation sciences	1. What are the optical and microphysical properties of aerosols from various sources?
	2. What are the properties of convective clouds and how do aerosols modify them?
	3. How well do properties of aerosols obtained from remote measurements by AERONET, satellites, and ER-2 instruments compare with those measured in situ?
	4. What are radiative properties of cirrus clouds?
General atmospheric science	1. What can be learned from polarimetric measurements?
	2. What can be learned by merging satellite and in situ measurements?
	3. Can vertical profiles from TCCON be verified?
	4. Test flights or transit flights

Table 3. SEAC[4]RS Flight Calendar and Flight Goals

	Aircraft			Stratosphere Goal[a]			Troposphere Chemistry Goal[a]								Radiation Goal[a]				General[a]			
Date	ER-2	DC-8	Lear	1	2	3	1	2	3	4	5	6	7	8	1	2	3	4	1	2	3	4
1 Aug	X	X																				X
2	X	X																				X
5		X																				X
6	X	X			X							X		X			X		X	X		
8	X	X			X	X							X		X		X					X
12	X	X	X				X	X	X		X		X	X	X	X	X	X				
14	X	X		X	X	X	X	X	X		X	X	X		X		X		X	X		
16	X	X		X	X	X						X	X	X	X		X		X	X		
19	X	X										X	X	X	X		X	X	X	X		
21	X	X	X	X		X	X	X	X		X		X		X	X	X	X	X	X		
23	X	X	X				X	X	X		X		X	X		X			X	X		
26		X			X							X			X					X		
27	X	X		X	X	X						X	X		X		X			X		
30	X	X	X			X	X	X	X		X			X	X			X		X		
2 Sep	X	X	X	X			X				X		X			X				X		
4	X	X	X													X		X	X	X		
6	X	X			X		X	X	X		X	X		X							X	
9	X	X	X			X	X	X	X	X	X	X			X		X		X	X		
11	X	X	X			X	X	X	X		X	X	X	X	X	X	X	X	X	X		
13	X	X		X		X							X			X	X	X	X			
16	X	X	X	X		X	X	X	X		X	X		X	X	X						
17			X														X			X		
18	X	X	X			X				X	X		X	X		X	X	X				
21		X					X	X	X		X		X									
22	X		X												X		X		X			X
23	X	X		X		X						X		X			X		X	X	X	X

[a]The numbers in the second row refer to the questions listed in Table 2.

measurements to demonstrate that water vapor is transported into the midlatitude stratosphere by individual convective cells and by mesoscale convective systems. In addition, biomass burning (BB) smoke (including both aerosols and gases from biomass combustion) stands out as a tracer of direct injection, since smoke has a low background concentration in the stratosphere and upper troposphere. Biomass burning smoke is observed in the UTLS, and direct injection of BB smoke by pyrocumulonimbus clouds or deep convection into the UTLS is occasionally observed: most often at high latitudes where the tropopause is lower and also into the midlatitude overworld [e.g., *Fromm et al.*, 2000; *Fromm and Servranckx*, 2003; *Jost et al.*, 2004; *de Laat et al.*, 2012].

A key question for SEAC[4]RS is to determine the depth of injection into the stratosphere that can occur by isolated storms, or mesoscale convective complexes, and the role of large-scale monsoonal flow in facilitating the transport. The low ceilings of aircraft in most previous airborne observations and the lack of targeted sampling limited the investigation of these water perturbations to relatively low altitudes. SEAC[4]RS used the high-altitude NASA ER-2, as well as balloon launches, to search for evidence of injections of water vapor across the tropopause by mesoscale convective complexes (MCCs), by tropical storms and hurricanes, and by individual convective systems.

The occurrence of MCCs peaks in the U.S. in June and July, with about seven or eight storms in these months in a typical year, though five or six storms occur on average in August [*Ashley et al.*, 2003]. They typically initiate at night and last fewer than 10 h. Because of their small numbers, difficulty in predicting them well in advance, and short duration, it is difficult to plan flights to intersect them even though they tend to occur most frequently in Texas and the states just to the north and east of Texas where they may contribute 20% or more of the seasonal rainfall. SEAC[4]RS did encounter several MCCs, and at least one of these, on 27 August 2013, was accompanied by high water vapor values in the lower stratosphere. There were few hurricanes in 2013, but in mid-September the outflow from Tropical Storm Ingrid, which eventually became a hurricane, was sampled. The inflow and outflow regions of numerous individual convective cells over the Southeastern U.S., and downwind of such cells in the North American Monsoon were also sampled. SEAC[4]RS has a useful data set for examining direct injection into the UTLS.

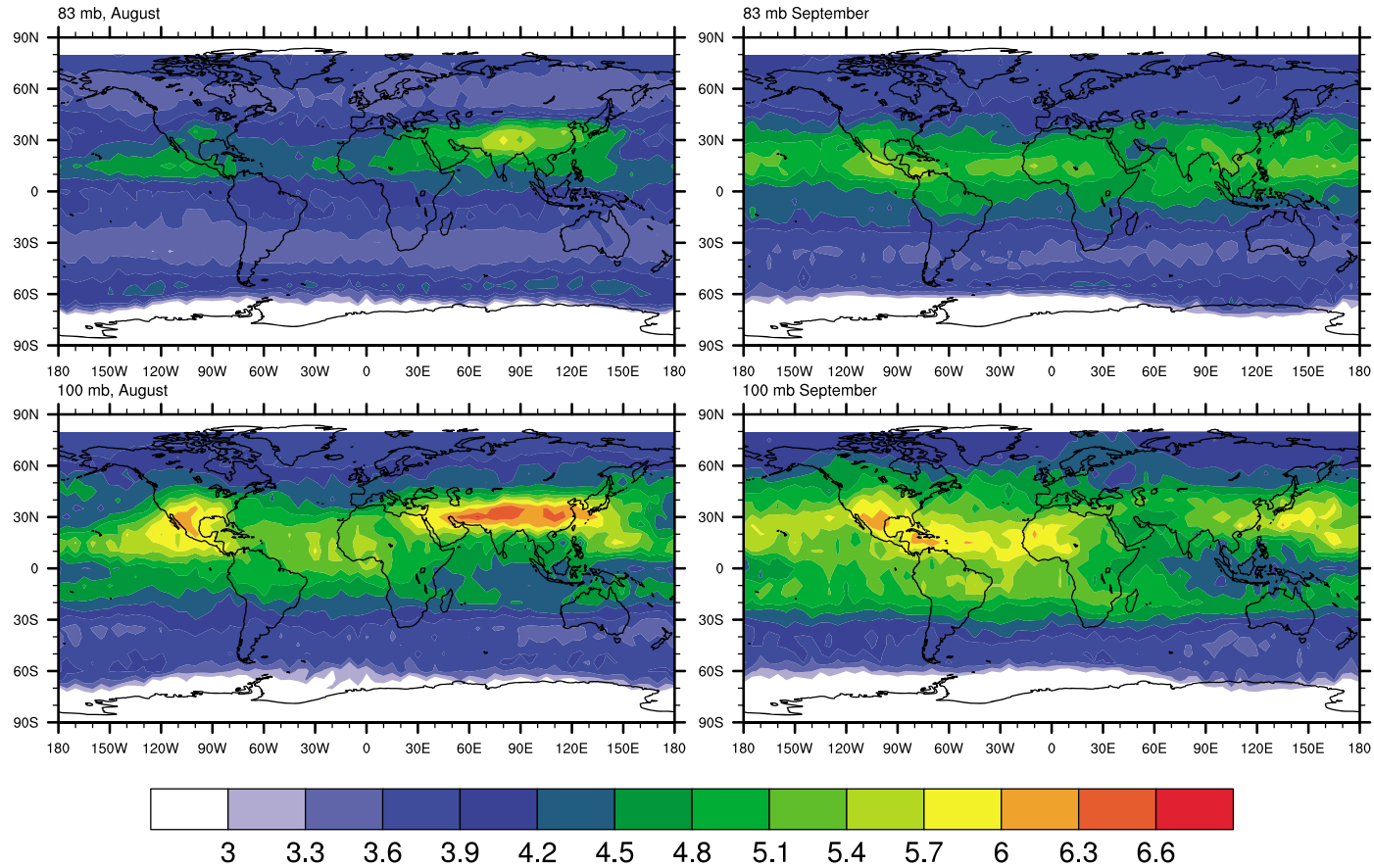

Figure 1. Microwave Limb Sounder measurements of water vapor (ppmv) at 83 hPa and 100 hPa for August and September 2013.

2.1.2. What Role Does the North American Monsoon Play in Transporting Water Vapor and Pollutants Into the Lower Stratosphere?

Air enters the stratosphere primarily in the tropics [e.g., *Holton et al.*, 1995; *Schoeberl et al.*, 2013]. Satellite observations, however, show evidence that the subtropical and midlatitude regions of the Asian Monsoon and the North American Monsoon (NAM) are also pathways [e.g., *Randel et al.*, 2010]. This transport signature is highlighted by water vapor observations.

Figure 1 shows the water vapor distribution as measured by the Aura Microwave Limb Sounder (MLS) [*Read et al.*, 2007] at two pressure levels during the SEAC^{4}RS mission in 2013. The 100 hPa pressure level corresponds to a pressure altitude of about 16 km, while 83 hPa corresponds to about 17.4 km, so these pressure levels approximately straddle the tropical tropopause. The geographic patterns of water vapor mixing ratio vary somewhat from year to year, but the general pattern is repeatable. In August of 2013 water vapor at 100 hPa was enhanced relative to the Northern Hemisphere tropics by about 30% in the Asian Monsoon region stretching over Asia and the Middle East, and by about 15% in the North American Monsoon region extending over Mexico, the Southwest U.S., and surrounding regions. In September 2013 at 100 hPa, the Asian summer monsoon signature has vanished, while the region of high water vapor associated with the North American summer monsoon is no longer very distinct. At 83 hPa, both monsoon circulations have enhanced water vapor in August, while in September the Asian Monsoon signal has vanished and the NAM has become part of a water anomaly that spans most of the Northern Hemisphere subtropics.

While the two monsoons have similar water vapor features in the UTLS, they differ in many other respects. The heavy isotope of water is considerably enhanced in association with the North American Monsoon, but not for the Asian Monsoon during June–August [*Dessler and Sherwood*, 2003; *Randel et al.*, 2012]. This difference is thought to be due to differing meteorological features. The NAM region has lower UTLS relative humidity than the Asian Monsoon region. As a result, more evaporation of convective ice, which is enriched in the heavy

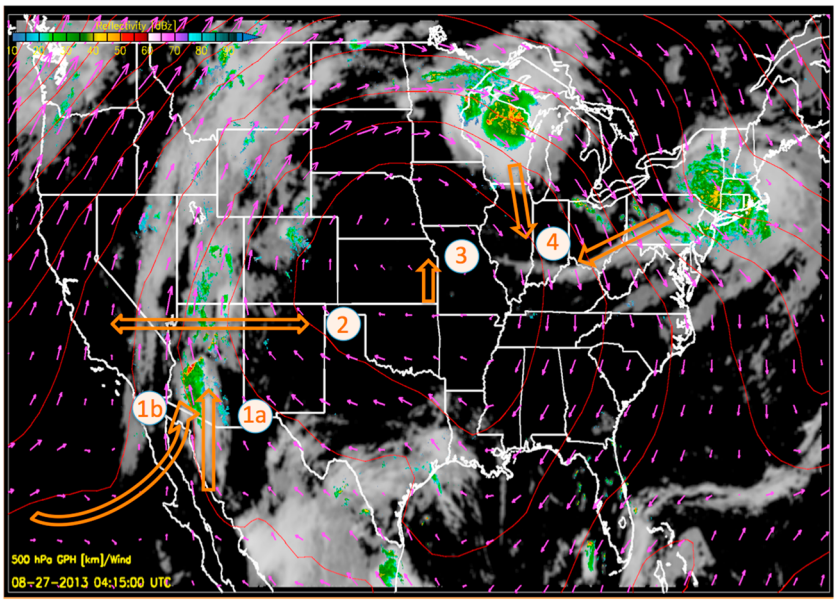

Figure 2. Dynamical setting of NAM circulation on 27 August 2013 and key elements of NAM flight planning. The figure includes GOES IR cloud information and national composite of NEXRAD radar reflectivity at 0400 UTC, together with the 500 hPa geopotential height (contours) and winds (arrows). The numbers and arrows refer to various interesting portions of the NAM. Labels 1a and 1b indicate an inflow region where two air masses merge. Label 2 indicates a region with a strong gradient in tropopause height at the edge of the monsoon. Label 3 is near the center of the monsoon. Label 4 indicates a region that is perturbed by mesoscale complexes.

isotope, may occur there leading to a larger input of water vapor that has been enriched in the heavy isotope in the convection [*Dessler et al.*, 2007; *Randel et al.*, 2012].

Satellite observations and models show that CO is enhanced, HCN is enhanced, and ozone is depleted in the UTLS over Asia but not over North America during the summer monsoon period [*Park et al.*, 2007; *Randel et al.*, 2010]. These enhanced concentrations of pollutants in the Asian Monsoon anticyclone are consistent with the strong local sources of pollution in Asia, which are largely absent in association with the NAM. The fact that ozone is not depleted in association with the NAM possibly reflects less meteorological confinement in the NAM as compared to the Asian Monsoon anticyclone. *Vernier et al.* [2011], *Thomason and Vernier* [2013], and *Vernier et al.* [2015] use CALIPSO, SAGE II, and balloon data to show that the highest aerosol optical extinctions near the tropopause occur in the Asian and North American Monsoon anticyclones. The NAM has a much weaker aerosol layer, the North American Tropopause Aerosol Layer or NATAL, than that found in Asia. Aircraft data from CARIBIC (Civil Aircraft for the Regular Investigation of the atmosphere Based on an Instrument Container) show that organic aerosols dominate at the base of the Asian Tropopause Aerosol Layer (ATAL) though sulfate aerosols are also present. Modeling by *Yu et al.* [2015] is consistent with the observations in the ATAL, but suggest that in the ATAL both primary and secondary organic aerosols are important, while in the NATAL secondary organics dominate.

SEAC^{4}RS flights explored the NAM region on seven flight days noted in Table 3. Regular balloon launches were also made. For 2013, the NAM circulation was active by the end of July and beginning of August, right before the beginning of SEAC^{4}RS. The effect of the NAM during that time period was captured by the transit flight on 8 August. During the first 2 weeks of the SEAC^{4}RS mission, the anticyclone was weak, but it reamplified during the third week of August. Figure 2 provides a description of the logic behind the flights that were focused on better understanding the vertical distributions of tracers across the tropopause and the contrast in atmospheric composition between the NAM anticyclone and the atmosphere external to the NAM. The anticyclone is highly variable, and Figure 2 provides just one example of its configuration. Further discussion of variability is provided in section 3 of this paper.

As indicated in Figure 2, the anticyclonic circulation brings warm and moist air masses into the continental U.S. (CONUS), generating convection of various scales in the region of the flow [*Minschwaner et al.*, 2015].

A number of key elements are marked on the figure, each associated with specific scientific objectives targeted during the NAM flight planning.

As shown in Figure 2 labels 1a and 1b, the southerly monsoonal flow entering the southwest U.S. is a merged flow from northern Mexico and from the Tropical Pacific. The air mass composition from the two origins is expected to be very different. The objectives of sampling this part of the flow, targeted on 16 August using both aircraft, were to identify the polluted and clean air masses entering the CONUS associated with the flow, the vertical distribution of the impact, and the mixing structure.

Associated with the NAM anticyclone are strong horizontal gradients in the UTLS, including tropopause height gradients. As discussed further in section 3, below, the tropopause height was generally typical of the tropics within the center of the anticyclone flow. One of the objectives of NAM flights was to quantify the gradients in UTLS composition, including water vapor, by sampling the chemical gradient across the monsoonal flow and the vertical gradient in the UTLS in the region of the flow. This objective, explored by paths such as label 2 in Figure 2, was successfully targeted on 8 August by both the ER-2 and the DC-8.

It is well documented using satellite data that the Asian summer monsoon (ASM) anticyclone has a strong signature of enhanced boundary layer tracers in the UTLS [e.g., *Park et al.*, 2007; *Randel et al.*, 2010]. The strong NAM-related convection in the central and northern plains (for example, noted in the enhanced radar reflectivity over Arizona, Utah, Colorado, Wisconsin, and Michigan in Figure 2) is energetic enough to produce tropopause-penetrating storms, injecting boundary layer species and water vapor into the lower stratosphere. Labels 3 and 4 on Figure 2 indicate paths to look for mesoscale convection injections over Wisconsin and Michigan. One of the NAM UTLS's study objectives was to investigate the effectiveness and the chemical signature of the injection. This objective was successfully targeted using ER-2 flights, especially on 8 and 27 August.

2.1.3. What Are the Water and Tracer Distributions in the Lower Stratosphere?

Another goal of SEAC^{4}RS was to determine the large-scale distributions of water vapor and trace gases in the UTLS during August and September. One measurement objective was to determine the structure of the NAM over the U.S. and to search for injections of tropospheric material into the stratosphere as discussed in sections 2.1.1 and 2.1.2. A second objective was to examine the general structure of the upper atmospheric composition during the time frame when summer transitioned to fall. As discussed in section 3 of this paper, the tropopause was generally above 15 km over the middle portion of the U.S. during the SEAC^{4}RS period, related to the fact that the subtropical jet was located near the Canadian border, so that subtropical stratospheric air extended far to the north of our base of operations in Houston, Texas. Such high tropopause values are common during summer. Lower tropopause altitudes near 10–12 km (typical of midlatitudes) were usually found over the extreme Western U.S., and the Northern U.S., although on many occasions midlatitude tropopause heights were only found north of the Canadian border. This structure was sampled several times during the mission. SEAC^{4}RS flew three long flight legs with the DC-8 and ER-2 over longitudes from Houston to California, to examine gradients of stratospheric constituents. One ER-2 flight after mid-September profiled the stratosphere from Houston to the Caribbean Sea off the coast of Nicaragua, while another sampled stratospheric air from Houston to Southern Canada and then to NASA's Armstrong (formerly Dryden) Flight Research Center in California. The DC-8 did similar flights at maximum altitude from Canada to Houston, and on its return from Houston to NASA Armstrong. Balloon launches were also conducted at several sites as described in section 4.2 of this paper.

2.2. Tropospheric Chemistry

As noted in Table 2, SEAC^{4}RS had a number of questions related to tropospheric chemistry. Generally, these fell into categories of understanding how the chemical environment was changing in time, the interactions between biogenic and anthropogenic emissions that drive ozone and aerosol chemistry, determining the properties of smoke from multiple types of fires, better understanding organic aerosols and gases, sampling different emission sources, and characterizing the vertical transport of chemical species by convection. Particular focus was placed on sampling a range of chemical regimes in the Southeast U.S. Dedicated flights were also conducted to sample fire plumes in the western U.S. SEAC^{4}RS interacted with the DISCOVER-AQ program, which sought to characterize the air pollution in the Houston region during September 2013. It also provided a chronological continuation of the Southeast Atmosphere Study field campaigns, which investigated air chemistry in the Southeastern U.S. during June and July 2013.

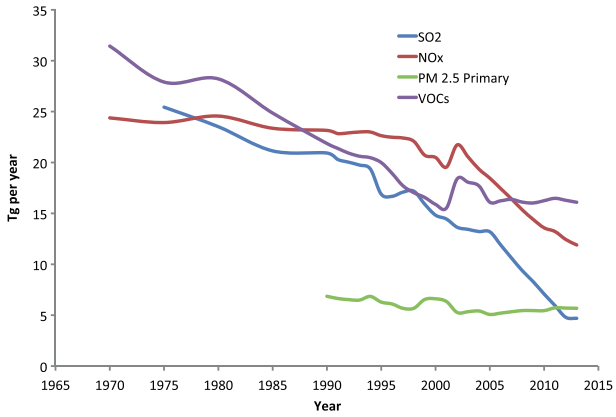

Figure 3. Anthropogenic emissions of various pollutants in the U.S. between 1970 and 2011 [*EPA*, 2014]. The VOC emissions include wildfires.

2.2.1. How Has the Chemistry Changed Over the Southeastern U.S. as Pollution From NO_x and SO_2 Declined?

Due to air pollution controls, and conversion of coal-fired power plants to natural gas, atmospheric chemistry has changed markedly over the U.S. during the past several decades. During this period nationwide ozone levels have declined by some 20%. Figure 3 illustrates trends in emissions of SO_2, NO_x, VOCs, and PM2.5 primary particles [*Environmental Protection Agency* (*EPA*), 2014]. These emission data include sources from fires but do not include biogenic sources of VOCs. Biogenic emission inventories and observations of formaldehyde (HCHO) from space show that the summertime emission rates of isoprene in the Southeast U.S. are among the highest in the world [*Millet et al*., 2008; *Guenther et al*., 2012].

Perhaps the most notable changes in emissions have been in NO_x and SO_2, both of which have been subject to emissions controls. Relative to 2000, SO_2 emissions fell by about a factor of 3, and NO_x emissions by about a factor of 2 by 2011. These trends in emissions are matched by trends in gas and aerosol concentrations. *Hidy et al*. [2014], for example, discuss concentration data from the Southeastern Aerosol Research and Characterization, SEARCH, sites. These data from 1999 to 2013 show concentration trends for a wide variety of species that are much like the emission trends illustrated in Figure 3. While trends varied between SEARCH sites, the sulfate concentrations averaged over all sites and the SO_2 concentrations at rural sites each fell by a factor of about 2 over the decade from 2000 to 2010, roughly in proportion to the change in SO_2 emissions over the same time frame in the region of the SEARCH sites. During this time period NO_y concentrations also fell by about a factor of 2, roughly in proportion to declining NO_x emissions in the region of the SEARCH sites.

Based on the changing emissions illustrated in Figure 3 one expects that aerosols over the U.S. are increasingly composed of organics that have a large biogenic component. The NASA DC-8 in SEAC^{4}RS carried a number of instruments designed to speciate the aerosols, helping to better understand their physical and optical properties and how they depend on particle composition. Instruments were also used to trace the conversions of biogenic gases into organic aerosols. SEAC^{4}RS also sampled occasional plumes of dust from the Sahara or more often plumes from western wildfires and southeastern agricultural fires.

Since NO_x is involved in important photochemical reactions in the atmosphere, its trends have implications for a range of species from ozone to organic gases and aerosols. NO_x concentrations drop off significantly in regions away from strong sources, so one can explore the chemistry of these species as a function of NO_x abundance by flying from relatively unpolluted regions to polluted ones. SEAC^{4}RS sampled environments with a large range of NO_x concentrations, providing an opportunity to explore the dependence of photochemical processes on NO_x. There is substantial uncertainty in the mechanisms of ozone and aerosol formation over the southeastern U.S., and models disagree greatly [*EPA*, 2011]. SEAC^{4}RS was focused on addressing many of these mechanistic shortcomings.

2.2.2. How Does the Seasonal Transition From Summer to Fall Impact Atmospheric Chemistry in the U.S. Southeast?

In addition to the decadal changes in the various gases and particles illustrated in Figure 3, there are also seasonal trends as illustrated in Figures 4 and 5. The seasonal trends from August to October generally are related to the relatively cooler temperatures and lower relative humidities in September and October than in August as discussed in section 3 of this paper. Biogenic VOC emissions are known to increase rapidly (doubling every 6–7°C) with temperature; oxidation chemistry is further enhanced under warmer and moister conditions. In addition, some plants begin to lose their leaves and become dormant for the winter starting in September.

Figure 4 shows that aerosol optical thickness (AOT) measured by MODIS (Moderate Resolution Imaging Spectroradiometer) in the Western U.S. declined by about 50% in magnitude but maintained a similar

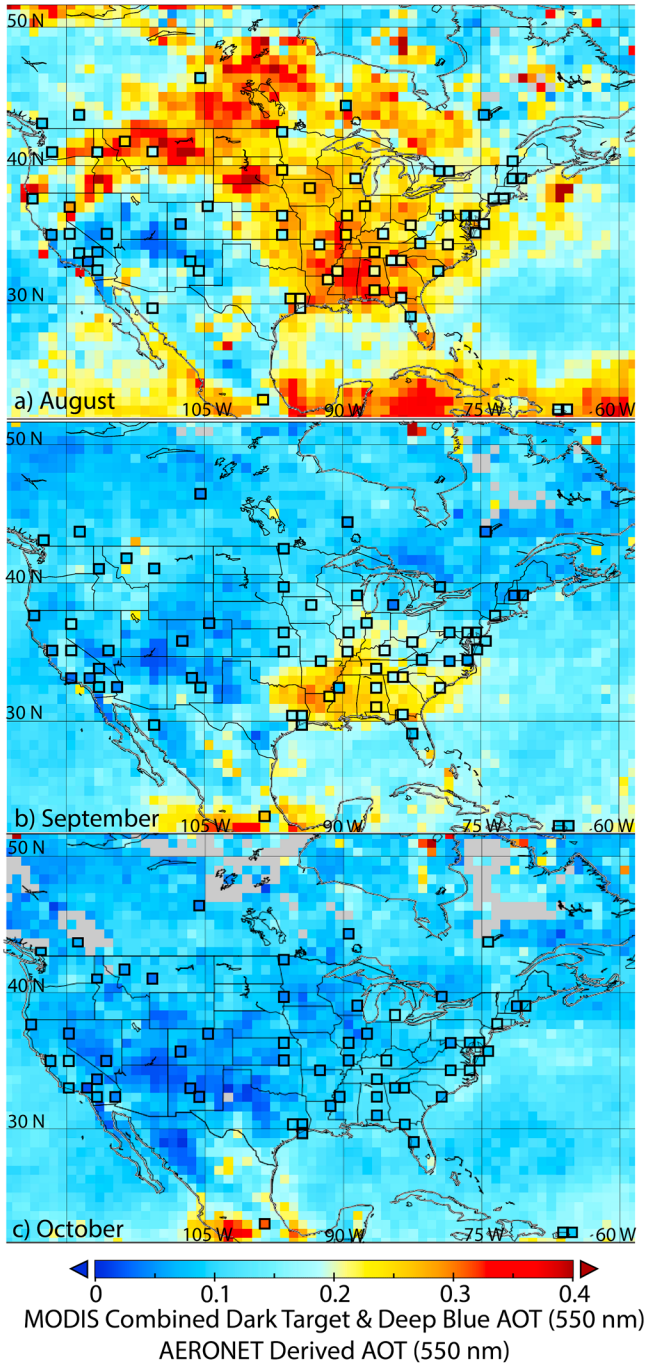

Figure 4. MODIS optical thicknesses for August, September, and October 2013 are shown in the background colors. AERONET monthly average optical thicknesses are shown in the boxes outlined in black.

geographic pattern between August and October 2013. The main source of the changing optical thickness in the Western U.S. is the seasonal decline in wildfires. The optical thickness over the Great Plains declined by about a factor of 5 between August and September, because fewer fires occurred in the regions of the west that are upwind of the Great Plains. Optical thickness in the Southeastern U.S. dropped by more than 25% from August to October 2013. The decline may be due in part to the seasonal ebb of biogenic VOC emissions and in part due to the weaker photochemistry for sulfate formation [*Kim et al.*, 2015].

Figure 5 illustrates measurements of formaldehyde from the OMI satellite instrument. Formaldehyde observed from space over the U.S. is a proxy for emission of isoprene, the dominant biogenic VOC [*Millet et al.*, 2008]. Figure 5 shows that the formaldehyde column density is highest in the U.S. Southeast, and concentrations decline from August to October. A major goal of SEAC^{4}RS was to investigate the seasonally changing chemical regime as isoprene decreases.

2.2.3. Can Isoprene Levels be Inferred From Satellite Measurements of Formaldehyde?

Formaldehyde is measured from space by solar backscatter around the 340 nm absorption band [*Chance et al.*, 2000]. Its main source in the eastern U.S. in summer is oxidation of isoprene [*Millet et al.*, 2006]. Anthropogenic sources are small in comparison and are only marginally detectable on the ~10 km pixel scale of the satellite data [*Zhu et al.*, 2014]. A number of studies have used formaldehyde measurements from space to quantitatively derive isoprene emissions [*Palmer et al.*, 2003, 2006; *Millet et al.*, 2008; *Barkley et al.*, 2013], but the measurements have never been properly validated. There is also large uncertainty in the isoprene-formaldehyde relationship, particularly at low NO_x [*Marais et al.*, 2012, 2014]. Observations of formaldehyde from space were available during SEAC^{4}RS from the OMI, GOME-2, and OMPS sensors, and two independent formaldehyde measurements were made from the DC-8 aircraft (Table 4). Validating the satellite HCHO data and better quantifying its relationship to isoprene emission under different NO_x regimes was a major achievement of SEAC^{4}RS.

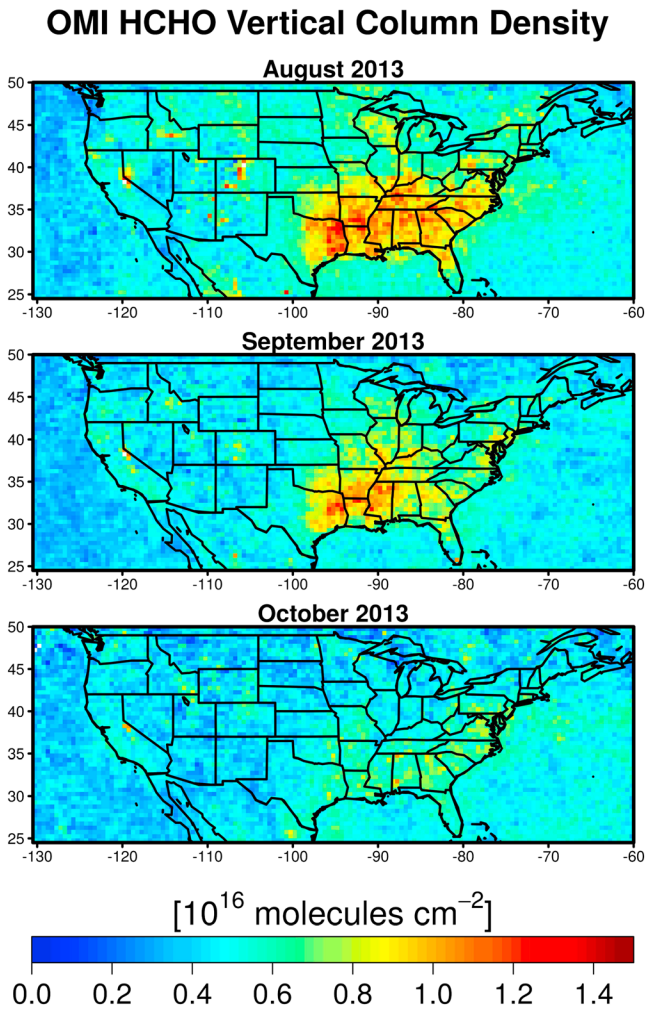

Figure 5. Monthly averages of formaldehyde observed by the OMI instrument from August to October, 2013. The large decline between August and October indicates a general seasonal trend in organic emissions. Figure courtesy of Lei Zhu.

In addition, SEAC^{4}RS data offer an ideal opportunity to test and validate models of biogenic VOCs emissions of a large variety of species such as isoprene, terpenes, alcohols, and carbonyls, many of which remain poorly quantified [*Guenther et al.*, 2012].

2.2.4. Is the Air Chemistry Significantly Modified Over Regions With Large Oilfields and Fracking?

Fracking (hydraulic fracturing), the production of oil and natural gas (methane) by the injection of fluids into the ground, may release methane, a potent greenhouse gas, and VOCs. Oil and natural gas production in older developed fields may also vent methane and VOCs. Evidence is mounting that different fields have different characteristics in terms of frequency of leaks during development and production, fraction of total production released as methane, and the mixture of VOCs that are released.

While not a major goal of SEAC^{4}RS, the DC-8 performed low-altitude passes or vertical profiles over clusters of offshore drilling platforms on several flights over the Gulf of Mexico, and over active drilling being conducted in the Eagle Ford and Haynesville shale plays. A missed approach near Dallas may have provided access to boundary layer air impacted by emissions related to extraction/production in the Barnett shale formation.

2.2.5. What Are the Properties and Transformations of Organic Gases and Aerosols in the Southeastern U.S.?

The lifetimes of isoprene and many other VOCs are very short. For instance, in midmorning, the lifetime of isoprene may be only half an hour. A fraction of the VOCs are converted into secondary organic aerosols. The secondary organic aerosol mass can be substantial relative to other aerosols. Multiple lines of evidence show that organic aerosols are a large fraction of the global aerosol burden. Therefore, the production of organic aerosols from VOCs is important to quantify, and the pathways are important to understand. Notably, organic aerosols have very complex compositions, with vast numbers of compounds present, and the gas-phase chemistry creating these compounds, or modifying them once present, is poorly understood. For these reasons the DC-8 payload in SEAC^{4}RS, discussed in section 4.1 and Table 4, contained many instruments designed to measure and speciate primary organic aerosols, emitted, for example, by fires, as well as VOCs and the secondary organic aerosol produced from them.

It was suggested that the conversion of organic gases to aerosols might create an elevated layer of particles over the Southeast [*Goldstein et al.*, 2009; *Ford and Heald*, 2013]. These suggestions were based on observations that summertime optical thicknesses in the southeast are 2–3 times larger than winter ones, while surface

Table 4. DC-8 Instruments

Name	Technique	Primary Investigator	Products
4-STAR	Sky scanning spectrometer	P. Russell, NASA Ames	Aerosol optical thickness, water vapor column
AOP	Aerosol optical properties	C. Brock, NOAA	Aerosol extinction, absorption, particle size
APR-2	Dual frequency Doppler Radar	S. Tanelli, JPL	Reflectivity, precipitation, vertical velocity
AVOCET	IR spectroscopy of CO_2	A. Beyersdorf, NASA LaRC	CO_2
BBR	Broadband radiometers	A. Bucholtz, NRL	Solar and IR radiative fluxes and heating rates
CAFS	UV-Vis actinic flux	S. Hall, UCAR	Spectrally resolved actinic flux and photolysis frequencies
CAMS	Compact atmospheric multispecies spectrometer	A. Fried, UCAR	CH_2O
CIT-CIMS	Chemical ionization mass spectrometer	P. Wennberg, CalTech	HNO_3, organic acids
DACOM	Tunable diode laser spectroscopy	G. Diskin, NASA LaRC	CO, CH_4, N_2O
DASH SP	Differential aerosol sizing and hygroscopicity	A. Sorooshian, UAz	Hygroscopic growth factor
DIAL-HSRL	UV lidar	J. Hair, NASA LaRC	O_3, aerosol and cloud heights, aerosol extinction
DLH	Open path TDL	G. Diskin, NASA LaRC	H_2O
GT-CIMS	Chemical ionization mass spectrometer	G. Huey, Georgia Tech	SO_2, HCl, HO_2NO_2, PAN
HD-SP2	Laser-induced incandescence	R. Gao, NOAA	Black carbon mass, size, coating thickness, hygroscopicity
HR-AMS	Aerosol mass spectrometer	J. Jimenez, U. Colorado	Aerosol composition
ISAF	Laser-induced fluorescence	T. Hanisco, GSFC	CH_2O
LARGE	Aerosol spectrometers	B. Anderson, NASA LaRC	Particle size distribution, optical properties, CCN
MMS	Meteorological measurements system	P. Bui, NASA ARC	Temperature, pressure, winds
NO_y, O_3	Chemiluminescence	T. Ryerson, NOAA	NO_x, NO_y, O_3
PALMS	Single particle composition mass spectrometer	K. Froyd, NOAA	Particle composition
PI Neph	Polarized imaging nephelometer	J. Vanderlei Martins, UMBC	Aerosol scattering phase matrix
PT-RMS	Proton transfer mass spectrometry	A. Wisthaler, U. Innsbruck	Volatile organic compounds
SAGA	Mist CHAMBER, ion chromatograph, filter	J. Dibb, U. New Hampshire	HNO_3, sulfate, soluble ions
SPEC	Cloud particle probes	P. Lawson, SPEC	Four-particle probes covering sizes from 1 μm to 10 cm
SSFR	Solar spectral flux radiometer	S. Schmidt, U. Colorado	Solar spectral fluxes and heating rates
TD-LIF	Thermal dissociation laser induced fluorescence	R. Cohen, U. C. Berkeley	NO_2, alkylnitrates, peroxynitrates, $CH_3O_2NO_2$
WAS	Whole air sampler	D. Blake, U. C. Irvine	>70 trace gases
DC-8 CAM	Forward and nadir cameras	Rick Shetter, U. N. Dakota	Nadir and forward video

level concentrations of aerosol mass do not change so much. *Wagner et al*. [2015] use data from SEAC^{4}RS and SENEX to show that sulfates are significantly enhanced in the transition zone from the boundary layer to the free troposphere where organic aerosols and sulfates might form. However, the enhancement only increases the column optical thickness by 10%, which is too small to account for a significant aerosol optical thickness change with season. *Kim et al*. [2015] use SEAC^{4}RS data to show that the difference in seasonality between AOT and surface aerosol concentrations mainly reflects seasonal differences in boundary layer depth; a shallower boundary layer with the same surface concentration will have a lower optical depth. SEAC^{4}RS did observe many cases in which aerosols were elevated aloft due to long-range transport from wildfires in the Western U.S. and Canada.

Significant portions of 11 DC-8 flights during SEAC^{4}RS were devoted to studying some or all of the questions focused on chemistry in the Southeastern U.S. (Table 2). In nearly all instances, attempts were made to fly through gradients in the amount of anthropogenic pollution that was mixing with the rich regional mixture of biogenic emissions. Segments of eight different flights focused on the Ozarks in southeastern Missouri where extremely high emissions and concentrations of isoprene were expected and found. Likewise, four different regions expected to be prolific producers of terpenes were targeted. Many flights followed evolving smoke plumes from fires as discussed in section 2.2.6. In addition, many flights explored the vertical evolution of VOCs and aerosols. High-frequency measurements of VOCs above source regions allowed for vertical flux measurements to be made in some cases [*Wolfe et al*., 2015] and for monitoring the evolution of aerosols as they were produced from the VOCs.

2.2.6. How Do the Properties of Smoke Vary Between Wildfires in the Western U.S. and Agricultural Fires in the Mississippi Valley?

Biomass combustion is an important source of gases and particles to the atmosphere [*Akagi et al*., 2011]. Many fires occur in forested regions and may consume large amounts of fuel. However, agricultural and other prescribed fires, which may individually consume only modest amounts of fuel, also contribute significantly to gas and particle emissions because of the large number of such fires. One goal of SEAC^{4}RS was to investigate a range of fires burning varying types of fuels to better understand the dependence of emission properties

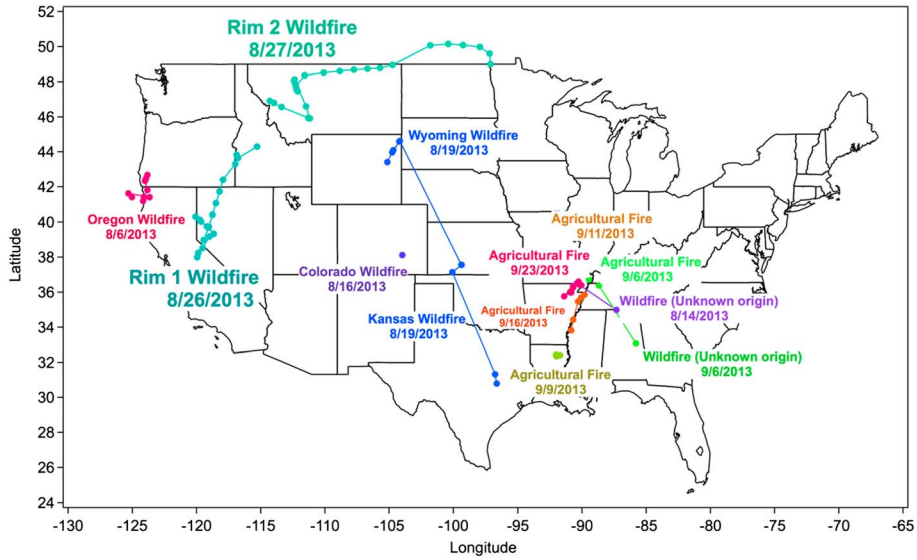

Figure 6. Location, date, and type of biomass fires and aged smoke plumes that were investigated as part of SEAC^{4}RS. The round symbols indicate locations where filters were collected on the DC-8 that were dominated by smoke from biomass burning. Lines connect filter-sampling locations on the same flight, and many instruments recorded continuous in situ smoke data in these areas. The ER-2 also collected remote sensing data on fires from above the DC-8 on 6 and 19 August. The text indicates the fire type (wild or agricultural) and (for most wildfires) the state where much/most of the sampling occurred. The Rim Fire (California wildfire) smoke was sampled on two consecutive days and mixed significantly with smoke from fires in ID and MT (not shown) on the second day (27 August). Figure courtesy of Rodney Weber.

on fuel type. Figure 6 illustrates the dates, locations, and types of fires that were investigated in SEAC^{4}RS. In addition to these fires, which generated distinct smoke plumes, the aircraft often encountered smoke from distant fires that burned in Oregon, California, Washington, and Idaho during 2013. The DOE's BBOP program measured a number of the same plumes as SEAC^{4}RS in the Northwestern U.S.

During the SEAC^{4}RS mission the Rim Fire occurred near Yosemite in California. The Rim Fire burned the third largest area in California's history, as discussed by *Peterson et al.* [2015]. The DC-8 aircraft was able to follow the smoke plume from its source, north to Idaho and then northeast into Canada [e.g., *Saide et al.*, 2015]. This is possibly the greatest distance over which a smoke plume has ever been followed. As it passed over Idaho and Montana the Rim Fire plume mixed to a possibly measureable extent with smoke from other fires, which can allow study of how plume mixing affects plume chemistry.

2.2.7. How Does Vertical Transport Modify the Chemistry of the Upper Troposphere?

A major goal of SEAC^{4}RS, in conjunction with the DC3 mission [*Barth et al.*, 2014], which shared much of the same payload on the DC-8 aircraft, was to investigate the roles of convection in transporting boundary layer materials into the upper troposphere and in removing, modifying, or producing chemical species during the transport. The Southeastern U.S. during summer experiences abundant convective storms often reaching well into the upper troposphere or even the stratosphere, as well as shallow convection that can link the boundary layer with the free troposphere. SEAC^{4}RS made a number of flights in which the radar on the DC-8 was used to characterize a convective cloud whose inflow and outflow were then sampled in situ by the DC-8 for chemistry and microphysics, the Learjet for cloud physics, and remotely by the ER-2. Often the DC-8 obtained samples in developing cells rather than in mature anvils. Different chemical species show different behaviors in response to convective cloud processes. For example, NO_x is produced in electrified clouds, so concentrations are higher in the outflow than the inflow. Soluble species, such as SO_2, are completely or partially removed in liquid clouds, while some products of aqueous chemistry such as sulfates are produced. Other species such as nitric acid can be trapped in ice crystals and then removed by falling ice. Understanding the behaviors of different compounds is a goal of SEAC^{4}RS.

2.2.8. What are the Air Quality Impacts of Urban Areas, Power Plants, and Other Localized Sources?

During SEAC^{4}RS there were many opportunities to characterize the outflow from urban areas and to investigate the interaction of the urban plume with surrounding air. Naturally, Houston was a focus of this activity.

Coincident with the latter part of SEAC^{4}RS, NASA's DISCOVER-AQ program was engaged in an intense study of Houston air quality. SEAC^{4}RS augmented these observations by obtaining cross sections of ozone in the urban area using the Ozone Differential Absorption Lidar (DIAL) system on the DC-8. SEAC^{4}RS also performed a number of air chemistry measurements above the Houston Ship Channel, which contains many hydrocarbon facilities. These flights provided detailed VOC signatures useful for apportionment of chemical emissions from these facilities. One flight module included multiple passes through the plume from the Houston Ship Channel at different ranges downwind to assess a long standing question about the relative importance of direct releases of HCHO versus photochemical production from alkenes released during routine operations as well as "upsets." Coordinated flights over various ground facilities, including balloon launching sites and AErosol RObotic NETwork (AERONET) sites, were made by both the DC-8 and the ER-2.

In addition to Houston, the DC-8 investigated the urban plumes from Birmingham, Alabama and Atlanta, Georgia. The DC-8 obtained vertical profiles over Dallas, Texas and Texarkana, Texas/Arkansas by doing missed approaches at the local airports on 16 and 23 August, respectively, while it flew through the plume of the Four Corners Power Plant on 16 August and sampled power plant impacts on the Ohio River Valley on numerous occasions. The DC-8 also investigated the air chemistry of the Central Valley in California, and of Fresno, California on 6 August. Los Angeles air chemistry was investigated as part of the final test flight on 5 August and again on 23 September when the DC-8 returned to base.

2.3. Radiation Sciences

2.3.1. What Are the Optical and Microphysical Properties of Aerosols From Various Sources?

The radiative forcing due to aerosol particles emitted over roughly a week (the typical particle lifetime) is a significant fraction, but generally with opposing sign, of the radiative forcing due to the greenhouse gases emitted since the industrial revolution. Better knowledge of aerosol properties is needed to determine the overall impacts. Lack of knowledge of the aerosol abundance and properties also prevents us from accurately determining the sensitivity of the climate to changes in radiative forcing. It is difficult to determine the aerosol characteristics because aerosols are complex and highly variable in time and space and have many properties that are important to characterize. As discussed in section 4 of this paper the DC-8 carried one of the most complete and advanced instrument packages for determining the characteristics of aerosols ever flown on a research aircraft. Particle physical properties such as size, composition, coating thickness, and abundance were measured. Particle thermodynamic properties, such as their interactions with water were measured. Also, aerosol optical properties such as optical thickness, wavelength dependence of optical thickness, scattering phase function, and single-scattering albedo were measured.

Many of the aerosol measurements from the DC-8 were coordinated with remote sensing measurements from the ER-2 and from AERONET sites.

2.3.2. What Are the Properties of Convective Clouds and How Do Aerosols Modify Them?

Vertical transport by convection is a principal means by which material in the boundary layer is vented into the free troposphere. Smaller, fair weather cumulus transport material through a transition layer into the lower free troposphere, as discussed in the context of SEAC^{4}RS by *Wagner et al.* [2015]. However, deep convective clouds, which were common during SEAC^{4}RS, can transport material into the UTLS.

Convective clouds can be modified by aerosols. Warm clouds are primarily impacted by the abundance of aerosols that often control the number of cloud droplets and their size. During SEAC^{4}RS there were many occasions when small cumulus were present at the top of the boundary layer. These clouds were observed in a variety of circumstances with varying types and amounts of aerosol. For example, an extensive set of such boundary layer clouds was present on the DC-8 flights through the smoke from the Rim Fire. Boundary layer clouds were also present over the Southeastern U.S. on many occasions. Due to their common occurrence, and significant fractional coverage, such clouds are radiatively significant and facilitate the pumping of boundary layer air into the lower free troposphere.

SEAC^{4}RS also observed many deep convective systems. The sampled deep convective systems occurred in a variety of aerosol environments over land and over the Gulf of Mexico. The clouds were characterized by the radar and lidar on the DC-8, as well as by ground-based lidars and radars, and by 5–15 min imagery from two Geostationary Operational Satellites (GOES). On several occasions the DC-8 and the Learjet sampled clouds near Huntsville, Alabama, where research radars were available to provide more information on the clouds.

One issue with comparing different clouds exposed to different aerosols in order to determine the impact of aerosols on clouds is the likelihood that the individual clouds are affected by the surrounding air masses whose thermodynamic or other properties differ along with the aerosols in the air mass. There were occasions during SEAC^{4}RS when local aerosol emissions, often due to fires, may have established varying aerosol abundance in an otherwise relatively homogeneous meteorological environment. These observations may help us better understand aerosol-cloud interactions. However, aerosol-cloud interactions are very complex, poorly understood, and cannot be fully resolved in one field mission.

2.3.3. How Well Do Properties of Aerosols Obtained From Remote Measurements by AERONET, Satellites, and ER-2 Instruments Compare With Those Measured In Situ?

Most of our knowledge of the global distribution and properties of aerosols comes from satellite remote sensing measurements. SEAC^{4}RS made numerous under flights of various satellite instruments in order to compare in situ data to that from the satellites and so that the satellite observations could provide spatial context for the suborbital SEAC^{4}RS measurements. Since satellites, other than geostationary ones, quickly pass over any point on the ground, the ER-2 was used as a surrogate satellite so that more prolonged remote sensing observations could be made while the DC-8 and the Learjet conducted in situ measurements to compare with and complement the remote sensing retrievals. Indeed, between the DC-8 and ER-2 research aircraft, SEAC^{4}RS flew the largest and most comprehensive remote sensing payload ever in a prolonged mission, with a spectral radiometer, three polarimeters, and two lidars. In addition, the 4-STAR airborne Sun and sky tracking photometer added another type of airborne remote sensing.

The synoptic AERONET network of Sun photometers installed for SEAC^{4}RS provides high-quality measurements of spectral column aerosol optical thickness as well as retrieved aerosol size and absorption properties for high AOT cases under good viewing conditions (AOT $>$ 0.4 at 440 nm; SZA $>$ 40°; uniform partly cloudy conditions or better). Therefore, many of the SEAC^{4}RS flights overflew one or more AERONET sites. Usually the DC-8 performed a "wall" pattern, which consisted of a series of legs of length about 100 km, stacked in altitude, above the AERONET site and under the ER-2, while the ER-2 flew a "rosette," or "clover leaf" pattern to give the remote sensing instruments views of the AERONET site at differing solar and viewing geometries.

One SEAC^{4}RS goal was to directly measure the single-scattering albedo under conditions when an AERONET site should have been able to retrieve it. Several such opportunities occurred during SEAC^{4}RS, mainly in situations where smoke was present and also over Houston. In addition, the 4-STAR instrument aboard the DC-8 made observations of sky radiances that can be inverted to provide AERONET-like retrievals of aerosol microphysical properties, thereby linking the AERONET ground-based observations more closely to the DC-8 aerosol in situ measurements.

2.3.4. What Are the Radiative Properties of Cirrus Clouds?

Cirrus clouds are important for the radiation budget and possibly for exchange of air between the troposphere and stratosphere. There were several occasions, noted in the individual flight descriptions below, when the DC-8 and Learjet sampled cirrus clouds over the Southeastern U.S. along the CALIPSO satellite track. During SEAC^{4}RS several flights were made into the tropics, and the ER-2 attempted to profile low optical thickness cirrus along the route, but few clouds were encountered. The complexity of the radiative properties of cirrus makes progress difficult. SEAC^{4}RS contributed to this data set, but it was not a major focus of the flights.

2.4. General Science Questions

2.4.1. What Can Be Learned From Polarimetric Measurements?

The ER-2 carried two polarimeters as part of a project to develop these techniques of measuring aerosol and cloud properties from space. These polarimeters were the Airborne Multi-angle Spectro Polarimetric Imager (AirMSPI) and the Research Scanning Polarimeter (RSP). On the majority of ER-2 flights, observations with the polarimeters were made over AERONET sites, or locations where the DC-8 or Learjet were present. Special flight paths were used to explore the observations with different Sun angles and to allow the polarimeters to scan the scene. Of particular interest was the flight on 6 August 2013, when instruments from both aircraft were able to observe and measure smoke properties above stratocumulus clouds. AirMSPI and RSP research teams are currently using these data sets to develop and evaluate aerosol and cloud products. For example, initial AirMSPI aerosol retrieval results for aerosol optical thickness, single-scattering albedo, and size distribution for a few cases are consistent with those derived from the AERONET and 4-STAR measurements. Initial RSP retrievals of cirrus cloud particle size, optical thickness, and asymmetry parameter compare favorably

with those derived from coincident eMAS retrievals. During SEAC^{4}RS the Passive Aerosol and Cloud Suite Polarimeter (PACS) group flew a portable imaging polarimeter (analogous to PACS) and the Polarized Imaging Nephelometer for data validation on board the NASA DC-8 aircraft. Both DC-8 instruments are being used for the development of aerosol and cloud retrievals for future satellite instruments as well as potential validation for the ER-2 polarimeters.

Evaluation of aerosol algorithms and aerosol properties retrieved from polarimeters in space will rely significantly on AERONET retrievals of column-averaged aerosol properties. SEAC^{4}RS measurements provide an opportunity to test the representativeness of the AERONET absorption retrievals for a limited number of cases with these high AOT as well as many other cases at lower AOT levels. SEAC^{4}RS data are being used to compare different techniques for measuring and retrieving aerosol absorption.

2.4.2. What can be Learned by Merging Satellite and In Situ Measurements?

During SEAC^{4}RS there were many opportunities to fly the aircraft in the viewing areas of various satellite instruments, other than those of the omnipresent low-resolution GOES imagers. Several special opportunities were sought and found. For instance, it is difficult to use passive remote sensing instruments to retrieve the properties of aerosols that have bright clouds or bright land surfaces below them. The ER-2 and DC-8 were fortunate to sample a stratus layer off the coast of Oregon and the forest fire smoke just above it on 6 August 2013. The ER-2 was able to make remote sensing observations, while the DC-8 measured these aerosols using both remote sensing (e.g., High Spectral Resolution Lidar) and in situ measurements. Satellite sensors in the NASA "A-Train" (e.g., MODIS, CALIOP) also acquired observations of this case of smoke above clouds. Another opportunity presented itself on our initial flight into Houston, when a layer of Saharan dust was present on 8 August 2013. Such dust is very common over the Atlantic, where it forms some of the highest optical thickness aerosol layers observed globally. This case presented the opportunity to measure this dust using both remote sensing and in situ instruments. In addition, SEAC^{4}RS was able to make observations of aerosol properties in a moderately dense wildfire smoke plume in conjunction with the MISR instrument on 19 August 2013 and also got a DIAL profile of smoke from the Rim Fire coincident with overpasses by AQUA and CALIPSO on 26 August. The combination of the satellite and aircraft data creates synergy that is useful for accurately constraining the aerosol properties measured in the context of a flight and ultimately using satellite remote sensing data to explore those properties globally.

2.4.3. Can Vertical Profiles From TCCON Be Verified?

The Total Carbon Column Observing Network (TCCON) is a global network of ground-based Fourier transform spectrometers recording spectra of the Sun in the near infrared. The goal of the network, initiated in 2004, is to measure the abundance of species such as CO_2, CH_4, N_2O, CO, HF, H_2O, and HDO to serve as a validation for the Orbiting Carbon Observatory and other related satellites such as GOSAT. A number of these species are measured in situ from the ER-2 and DC-8 platforms. The DC-8 and ER-2 aircraft performed targeted deep vertical profiles above TCCON sites to provide accurate measurements of key greenhouse gases (e.g., CO_2 and CH_4) with the goal of improving the accuracy of the TCCON-retrieved columns. During SEAC^{4}RS a TCCON station was set up at NASA's Armstrong Research Center, and another was present at the DOE Atmospheric Radiation Measurement Program Southern Great Plains site. Two profiles were made over the site at Armstrong, the first with only the DC-8 during the 5 August test flight and the second on 23 September, which combined ER-2 and DC-8 descents to yield a profile from the lower stratosphere to the ground. The DC-8 also did a spiral over the Southern Great Plains ARM site.

2.4.4. Test Flights or Transit Flights

At the beginning of SEAC^{4}RS a series of flights were made to test the instruments, as noted in Table 3. These test flights were also used to fine-tune joint flight maneuvers with the ER-2 and DC-8, to overfly a TCCON site and to sample urban pollution from the greater Los Angeles area. Transits to and from Ellington Field included scientific measurements, as also noted in Table 3.

3. Meteorological Context

SEAC^{4}RS took place during the late summer and very early fall—in essence during a transition period. During the summer, the equator-to-pole temperature gradient is weak, there are strong quasi-stationary large-scale troughs and ridges, and the traveling waves that generate winter storm patterns are relatively weak. As fall sets in, the equator-to-pole temperature gradient strengthens, the stationary patterns are less prominent, and the circulation is more strongly dominated by traveling waves.

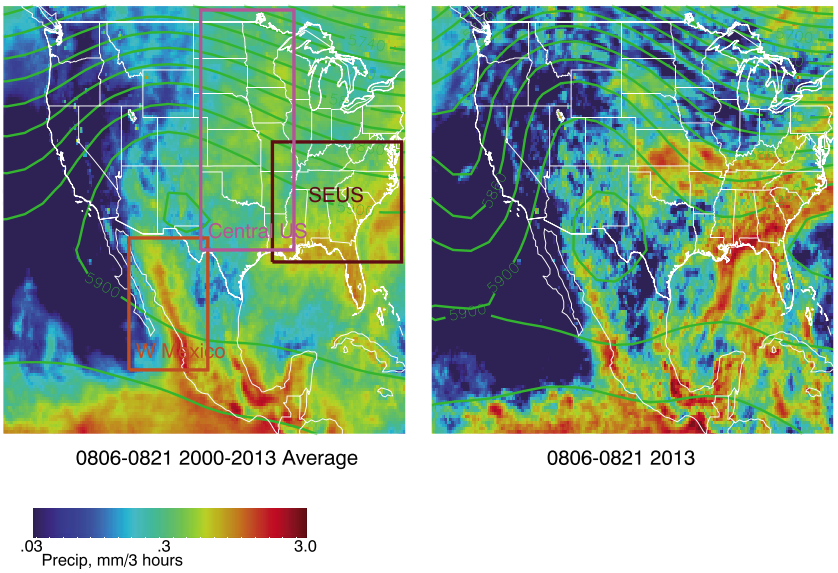

Figure 7. Rainfall rate (from the NOAA CMORPH data set) averaged over a 13 year period for the period (a) 6–21 August 2000, and for (b) 6–21 August 2013. The rainfall rate is in units of millimeters in 3 h averaged over the time period. Averaged 500 hPa heights from the NCAR-NCEP reanalysis data set are overplotted: 25 year averaged for 6–21 August 2000 (Figure 7a) and 6–21 August 2013 (Figure 7b). Colored rectangles in Figure 7a indicate specific sectors for which precipitation is plotted in Figures 10b–10d.

Precipitation in the SEAC^{4}RS region during the summer period is dominated by convective systems of a variety of regional types. Figures 7–9 show both the 13 year average rainfall in North America during three sequential 2 week periods that covered the SEAC^{4}RS field experiment (Figures 7a, 8a, and 9a), and the actual rainfall for those 2 week periods during SEAC^{4}RS (8 August 8 to 23 September 2013—Figures 7b, 8b, and 9b). As an indicator of the circulation, the respective 500 hPa geopotential heights are overplotted (using 25 year average NCEP-NCAR reanalysis data). Note that rainfall is used as a proxy for convection; this is reasonable during the summer months, where nearly all precipitation is convective in the SEAC^{4}RS region. During the first two periods (Figures 7 and 8), the most important feature of the 13 year average circulation is the strong ridge over the western U.S., due to the North American Monsoon driven by convection (and its associated

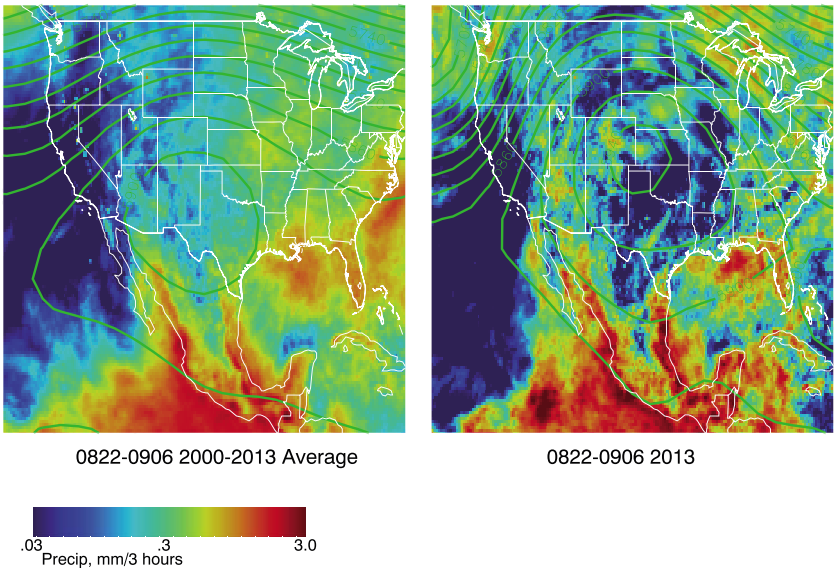

Figure 8. As in Figure 7 but for 22 August to 6 September.

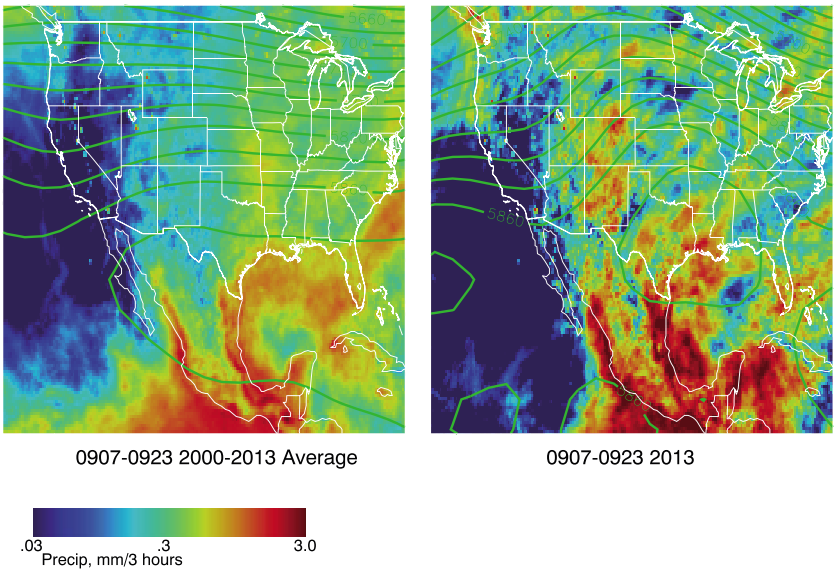

Figure 9. As in Figure 7 but for 7–23 September.

upper level divergence) in the mountains of western Mexico and in the southwestern U.S. On average, this ridge weakens somewhat during the second period (Figure 8a—maximum geopotential heights are lower), and by the middle of September (Figure 9a) is essentially absent, marking the demise of the strong stationary pattern and the advent of the fall and winter traveling wave patterns.

Convection during the late summer (Figure 7a) has several different distinct regional types. The Sierra Madre convection in western Mexico is highly concentrated, highly diurnal (maximum about 06:00 P.M. local time), and, except for the tropical systems to the south, is generally the deepest. This convection reaches into Arizona and New Mexico, to help produce the summer maximum in rainfall in those areas. As the summer ends and fall begins, this convection exhibits a clear retreat, essentially merging with tropical convection by mid-September (Figure 9a). Over the Central U.S., extending north into Canada, convection is dominated in the summer by large (100 km by 100 km or larger) mesoscale convective complexes that form in the late afternoon just east of the Rocky Mountain chain and propagate eastward during the night. These systems are less frequent as the transition to fall occurs (lower rainfall, Figure 10a): typically at the end of September there is an increase in rainfall, but this is due to traveling frontal systems. Over the southeast U.S. and Gulf of Mexico, convective systems are smaller; as elsewhere over land, the systems exhibit a clear diurnal character. Over land areas, the evolution of convection during the period is similar to behavior over western North America, with deep convection declining steadily as the season progresses. Over the Gulf, however, rainfall and convection increase during the early fall on a climatological basis, due to the maximum incidence of tropical cyclones that occurs in mid-September.

Figures 7b, 8b, and 9b show the average picture for convection and circulation during the SEAC4RS period. But how did the evolution of the basic meteorology differ from "typical" during the 2013 field experiment, specifically in quantities that affect the major science issues, including the North American Monsoon, chemistry in the southeast U.S., convection in the Gulf and the southeast, and the distribution of smoke from forest fires? Figure 10 shows a summary of how some of the bulk meteorological quantities related to these science issues varied during the experimental period and how that variation compares to an "average" year. For each bulk quantity (described below), the multiyear mean and standard deviation for each day is shown, along with the value for 2013. All the quantities are subject to a 7 day smoothing. The regions used for computing the precipitation bulk quantities are defined by the rectangles in Figure 7a.

The latitude of the maximum in 200 hPa geopotential height (assumed to be a proxy for the center of the anticyclonic circulation driven by the North American Monsoon convection) is shown in Figure 10a (the magnitude of the geopotential height maximum, not shown, exhibits a similar evolution). The most important feature is the unusually high latitude (and high strength) of the anticyclone during late August and early

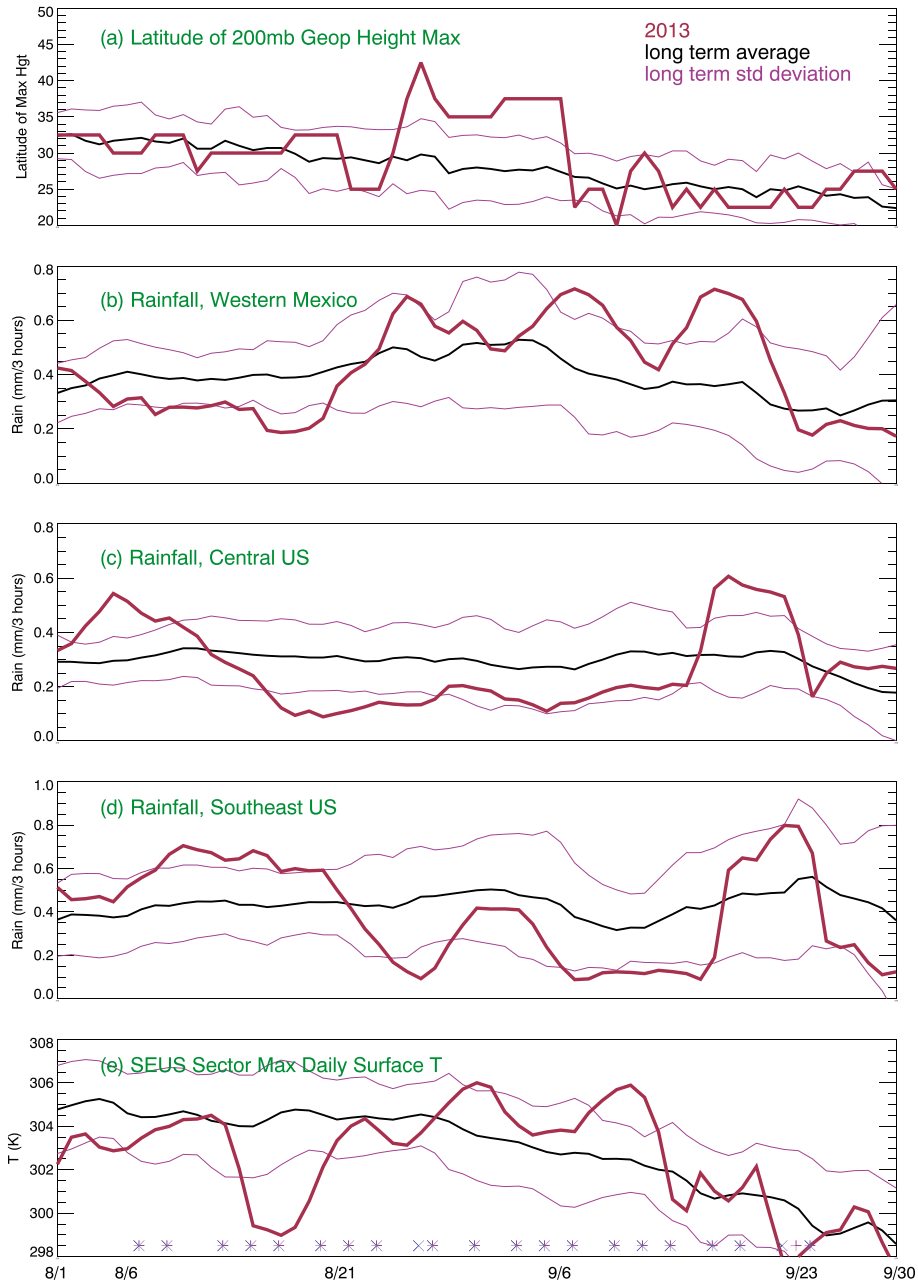

Figure 10. Fourteen year average quantities (2000–2013, black, standard deviation in magenta) and corresponding 2013 quantities (maroon) for August and September: (a) latitude of center of anticyclone in western North America (cf. Figure 7a); (b) rainfall in Western Mexico (orange sector in Figure 7a); (c) rainfall in the Central U.S. (yellow sector in Figure 7a); (d) rainfall in the Southeastern US (maroon sector in Figure 7a); (e) surface temperatures (station based) in the Southeastern U.S. The cross and plus symbols along the bottom of Figure 10e indicate flight days for the DC-8 and ER-2, respectively.

September (and its relative weakness during the first part of August). In fact, the center of the anticyclone is north of the mean by more than a standard deviation and is the most northerly position in 25 years of data. This anomalously strong ridge (which is clearly apparent at 500 hPa—cf. Figures 8a and 8b) contributed to the northerly track of the smoke from the Rim Fire that was surveyed on 26–27 August. Not surprisingly, western Mexico rainfall (Figure 10b) exhibits a corresponding pattern, with below average precipitation during early to mid-August (Figure 7b), rising to substantially above average precipitation during late August and early September (Figures 8b and 9b). There were five Pacific tropical cyclones in this region from 26 August to 15 September, which made significant contributions to the rainfall.

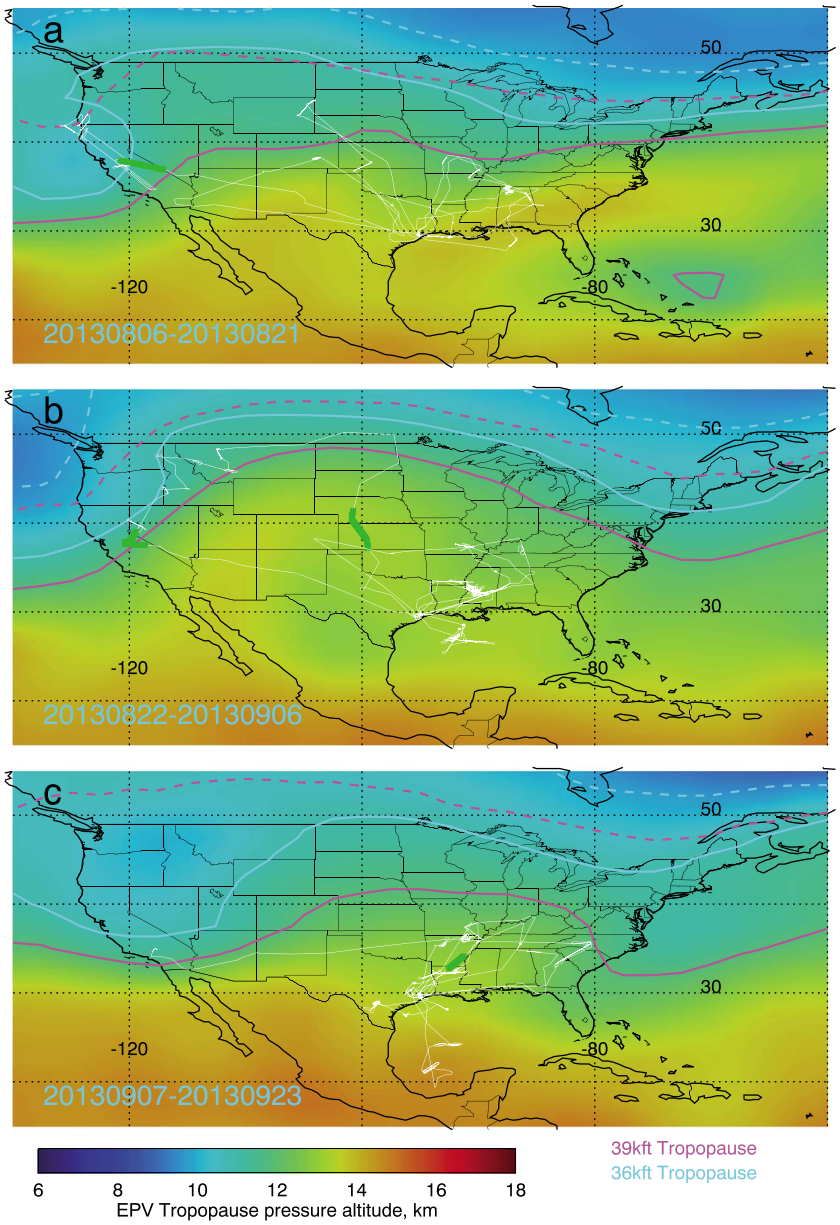

Figure 11. EPV Tropopause pressure altitude (using EPV of 2 PVU) for the (a–c) three periods defined in Figures 7–9 (2013 only). Also plotted are the DC-8 flight tracks during each period (white), as well as 36,000 ft (cyan) and 39,000 ft (magenta) contours for the EPV tropopause (solid) and the WMO tropopause (dashed). The contour lines are given in feet units to correspond to the pressure altitude of the DC-8. Its practical ceiling is 39 kft, which was rarely reached. Green portions of flight tracks represent sections where the analysis EPV interpolated along the flight track was greater than 2 PVU.

In the central U.S. (see rectangle in Figure 7a), the most notable feature is the anomalously low precipitation (Figure 10c) during much of the experimental period, reflecting fewer mesoscale convective complexes (MCCs) than average. To some extent (especially while the ridge was strong and displaced to the north—after about 23 August) this anomalously low rainfall is due to large systems being displaced north into Canada, beyond the range of the outlined rectangle in Figure 7a. However, except for the very earliest part of the experiment, midwestern MCCs were less frequent than typical. What this suggests is an important role for deep systems in Western Mexico in producing deep injections of water vapor into the stratosphere. Nevertheless, elevated water in the stratosphere due to MCCs was observed at least twice during the experiment. Note that the central U.S. rainfall enhancement in mid-September is from a frontal system.

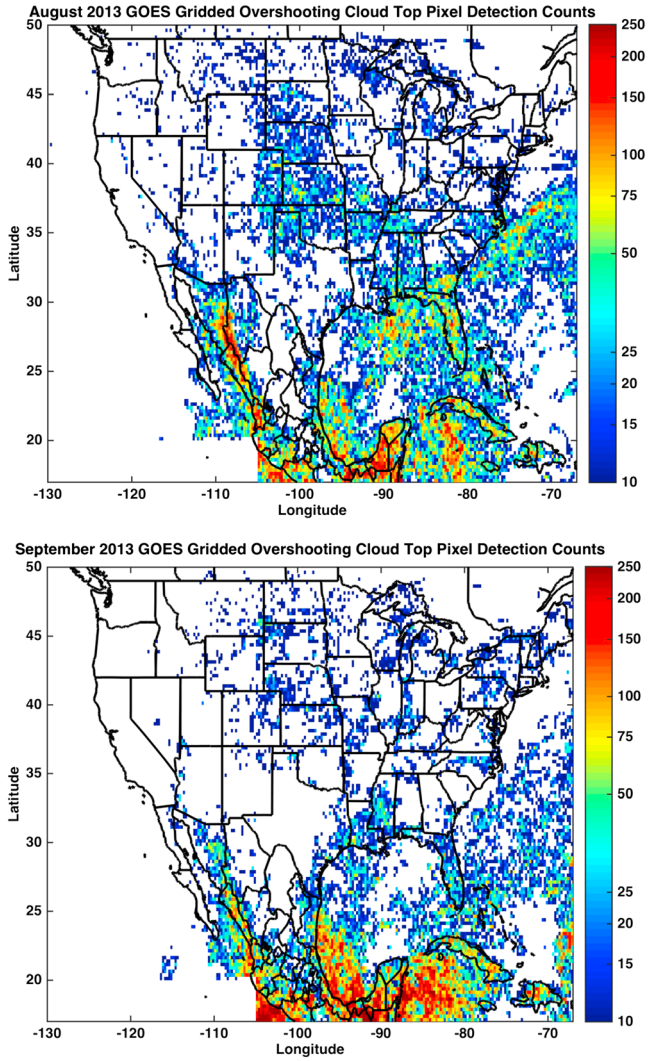

Figure 12. The number of overshooting convective cloud tops in August and September 2013 per 600 km^2 grid cell based on GOES observations (K. Bedka, private communication, 2016) (NASA LaRC).

In the Southeast the rainfall and maximum temperatures (Figures 10d and 10e) are anticorrelated (negative correlation of 0.77 at a 4 day lag) and related to Western Mexico convection (negative correlation of 0.87 with Southeast U.S. rainfall). Until about 23 August, conditions in the Southeast U.S. included a well-positioned weak trough that steered moist air into the region and provided the uplift to produce precipitation that was significantly above normal (Figures 7b and 10d). Temperatures were substantially colder than typical (Figure 10e). By the last week of August, though, a strong ridge emerged in the western U.S. (Figure 8b). It was displaced slightly east of its "average" position, yielding warm and stable upper level conditions over the southeast U.S. So, for about 2 weeks, conditions over the Southeast U.S. were warmer and drier than the averages (Figures 10d and 10e). Effectively, the beginning of the cooling trend in maximum temperatures in the Southeast U.S., which typically starts in the last week of August, was postponed nearly 2 weeks into mid-September. This pattern is also consistent with the anomalous ridge pattern at 500 hPa in the last 2 weeks of the experiment (Figure 9b).

Figures 11a–11c show the tropopause pressure altitudes for the three averaging periods defined in Figures 7–9 (2013 only) using the NCAR/NCEP reanalysis data. The figures include both the "tracer" tropopause (or EPV tropopause, defined by the Ertel potential vorticity surface of 2 Potential Vorticity Units (PVU)—solid lines *and* the color fill) and the "thermal" tropopause (or WMO tropopause, defined in terms of vertical temperature gradients—dashed lines). These two definitions of the tropopause can be considered as representing the bottom and center of the midlatitude tropopause transition layer, respectively [*Hoor et al*., 2002; *Pan et al*., 2004, 2007].

Perhaps the most important feature of the tropopause for the purposes of this experiment was that the WMO tropopause was largely above the effective ceiling of the DC-8 (39 kft, pressure altitude dashed line in the figures; although 40–41 kft pressure altitude can be reached for short durations). In fact, as shown by the limited number of green areas along the DC-8 flight tracks in Figure 11, there were only a few penetrations of the EPV tropopause, though ozone did exceed 100 ppbv at high altitudes a significant number of times (a good indicator of stratospheric influence). The basic structure of the evolution follows the 500 hPa pattern in Figures 7b, 8b,and 9b. Namely, in the earliest period (Figure 11a), the ridge is relatively weak, with a Pacific trough impinging to the west. The only significant stratospheric penetration during this period was a flight west toward this trough, which defined the western edge of the (anomalously weak) monsoon anticyclone. The western U.S. ridge became anomalously strong during the second period (Figures 8b and 10a), and this was reflected in the tropopause structure. Penetrations of the EPV tropopause occurred only during the

Table 5. ER-2 Instruments

Name	Technique	Primary Investigator	Products
AirMSPI	Multiangle spectropolarimetric imaging	D. Diner, JPL	Multiangle polarization images
ALIAS	Laser infrared absorption spectrometry	L. Christensen, JPL	CO, N_2O
BBR	Broadband radiometers	A. Bucholtz, NRL	Solar and IR radiative fluxes and heating rates
CPL	Lidar	M. McGill, NASA Goddard	Attenuated backscatter
eMAS	Multispectral scanning MODIS simulator	S. Platnick, NASA Goddard	Spectral images
FCDP	Optical particle sizing	P. Lawson, Spec Inc.	Particle size 1–50 μm
H2Ov	Lyman α + tunable diode laser	J. Anderson, Harvard	Water vapor
JLH	Tunable diode laser	R. Herman, JPL	Water vapor
MMS	Meteorological measurements system	P. Bui, NASA ARC	Temperature, pressure
MTP	Microwave radiometry	M.J. Mahoney, JPL	Temperature profiles
PCRS	Cavity ringdown spectrometer	S. Wofsy, Harvard	CO_2, CH_4, CO
RSP	Scanning polarimeter	B. Cairns, GISS	Multiangle polarization
SSFR	Solar spectral flux radiometer	S. Schmidt, U. Colorado	Solar spectral fluxes and heating rates
UAS-O3	UV photometry	R.-S. Gao, NOAA	Ozone
WAS	Whole air sampling	E. Atlas, U. Miami	>50 trace gases

flight to the Rim Fire at the western edge of the ridge, and on the return from the Rim Fire plume sampling, as the DC-8 flew at high altitude and sampled streamers of high EPV air that had been entrained into the ridge from higher latitudes. During the last 2 weeks, as the ridge weakened, the aircraft flew farther south than in the earlier periods, so penetrations were few even though the ridge pattern had weakened. Nevertheless, there were five instances of significant stratospheric influence during this period, when EPV exceeded 1.5 PVU and ozone was over 100 ppbv.

Satellite data can be used to identify clouds that are penetrating the tropopause. Figure 12 illustrates the number of pixels in a grid cell with cloud tops above the tropopause in August and September 2013 using imagery from GOES and the techniques developed by *Bedka et al*. [2010]. In parallel with the rainfall shown in Figures 7–9, Figure 12 indicates that hundreds of clouds penetrated the tropopause in each ~600 km^2 grid cell along Mexico's Sierra Madre Occidental Mountain range during August 2013. GOES makes about 1450 observations per grid cell in a month, so 200 cloud penetrations suggest that these features occur 14% of the time, or for approximately 3 h per day. Fewer clouds, but still in the range from 50 to 200 per 600 km^2 grid cell penetrated the tropopause over the Mexican mountains in September 2013. Another very active convective region is the northern Gulf of Mexico, Florida, and the southern portions of Mississippi, Alabama, and Georgia where 50 to 100 clouds penetrated the tropopause per 600 km^2 grid cell in August 2013. Figures 7–9 indicated this was also a region of heavy rainfall.

4. Implementation

4.1. Aircraft Payloads, Flight Coordination and Flight Paths

The payloads outlined in Tables 4–6 and Figures 13–15 were developed in order to address the goals discussed in section 2 of this paper. The DC-8 employed 23 in situ and 5 remote sensing instruments for radiation, chemistry, and microphysics as illustrated in Table 4 and Figure 13. The ER-2 employed seven remote sensing

Table 6. Learjet Instruments

Name	Technique	Primary Investigator	Products
2D-S	Optical array	P. Lawson, SPEC Inc	10 μm to 3 mm particle sizing
CPI	Digital camera	P. Lawson, SPEC Inc	2.5 μm pixel resolution cloud particle images
FCDP	Forward scattering	P. Lawson, SPEC Inc	2–50 μm size
FFSSP	Forward scattering	P. Lawson, SPEC Inc	2–50 μm size
HVPS	Optical array	P. Lawson, SPEC Inc	150 μm to 2 cm
Dew point	Chilled mirror	P. Lawson, SPEC Inc	Dew point temperature
LWC/TWC	Hot wire/Hot cone	P. Lawson, SPEC Inc	Liquid water/Ice water contents
Rosemount temperature	Total temperature	P. Lawson, SPEC Inc	Temperature
Rosemount icing rod	Vibrating rod	P. Lawson, SPEC Inc	Detect supercooled drops
AIMMS-20	3-D-air motion differential GPS	P. Lawson, SPEC Inc	3-D winds, position
NMASS	Differential CN counters	J.C. Wilson, U. Denver	4 nm to 0.1 μm particle sizing

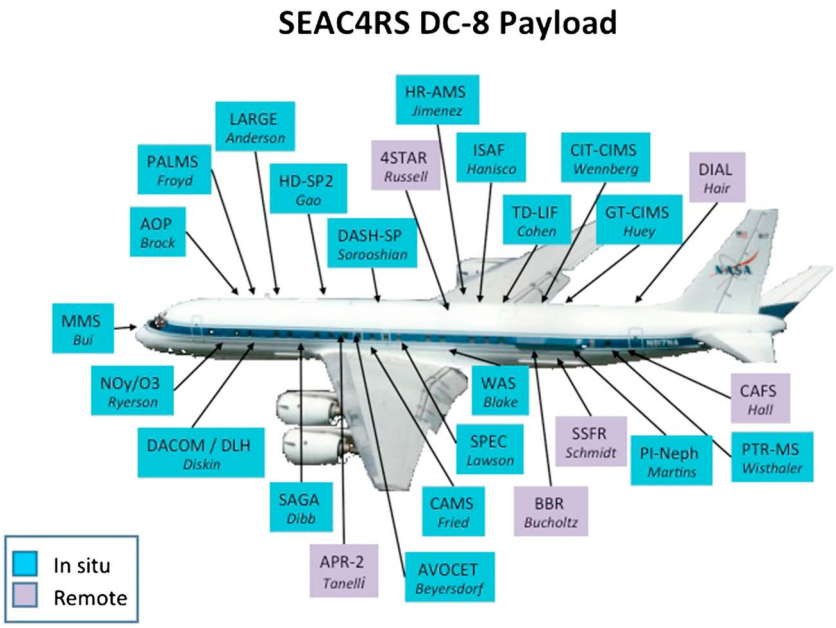

Figure 13. The approximate locations of the 27 instruments carried by the DC-8 during SEAC^{4}RS. Instruments in pink use remote sensing, while the other instruments make in situ measurements. The DC-8 also had a nadir and forward viewing camera.

instruments as a satellite surrogate, as well as eight in situ instruments as indicated in Table 5 and Figure 14. The Learjet had 11 instruments designed to measure the microphysical properties of clouds and precipitation, as given in Table 6 and illustrated in Figure 15. The reader should contact the primary investigators listed in the Tables for details concerning instrument performance and accuracy.

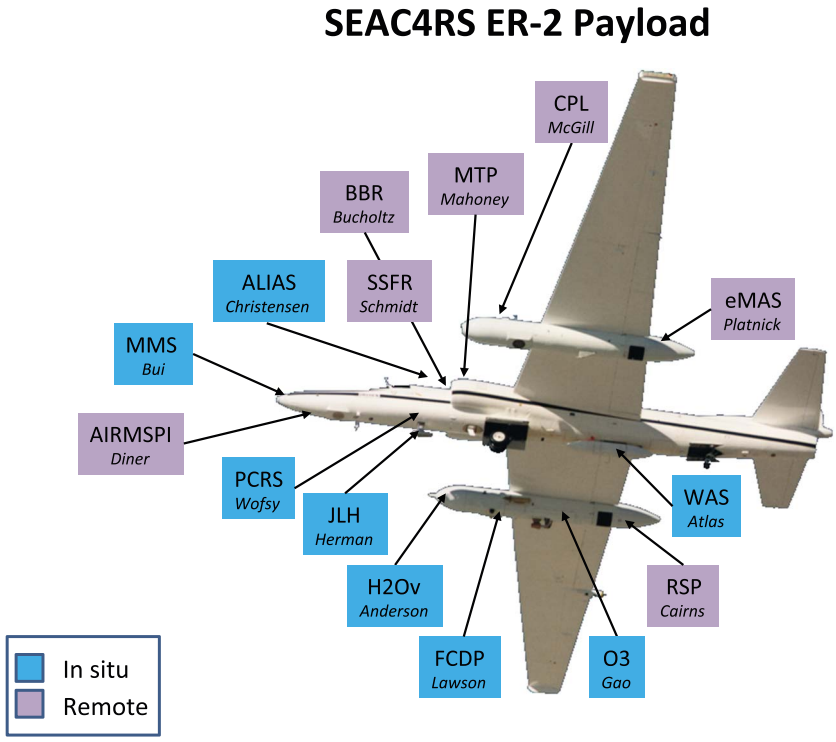

Figure 14. The approximate locations of the 15 instruments carried by the ER-2 during SEAC^{4}RS. Instruments in pink use remote sensing, while the other instruments make in situ measurements.

Figure 15. The approximate locations of the 11 instruments carried by the SPEC Learjet during SEAC^{4}RS. All the instruments make in situ measurements. Photo courtesy of Paul Lawson.

Figure 16 illustrates the cumulative flight hours flown by each of the three aircraft. SEAC^{4}RS generally enjoyed good weather and an absence of aircraft maintenance issues. On a few occasions the ER-2 returned to Ellington Field early due to the threat of afternoon thunderstorms. Because of the good weather and excellent aircraft performance, a large number of flights were made, many of which involved close coordination between the aircraft.

As in the CRYSTAL/FACE field mission [*Jensen et al.*, 2004] and the Tropical Composition, Climate and Chemistry Coupling, TC^4, mission [*Toon et al.*, 2010] and numerous other recent NASA field missions, the SEAC^{4}RS scientists were able to monitor the location of each aircraft in real time at the mission headquarters, located at Ellington Field. This monitoring allowed a flight control scientist, usually Karen Rosenlof, at Ellington Field to coordinate with the flight scientists for each of the aircraft, the mission meteorologists, the theory teams, a ground navigator for the DC-8, and an on-site pilot who in turn communicated with the pilots of the three aircraft. The flight control scientist could change flight plans in near-real time in response to evolving weather, to remote sensing data from satellites, to data from ground stations, or to the need to better coordinate planes, so that, for instance, the ER-2 remote sensing instruments were spatially aligned with the DC-8 and Learjet collecting in situ data.

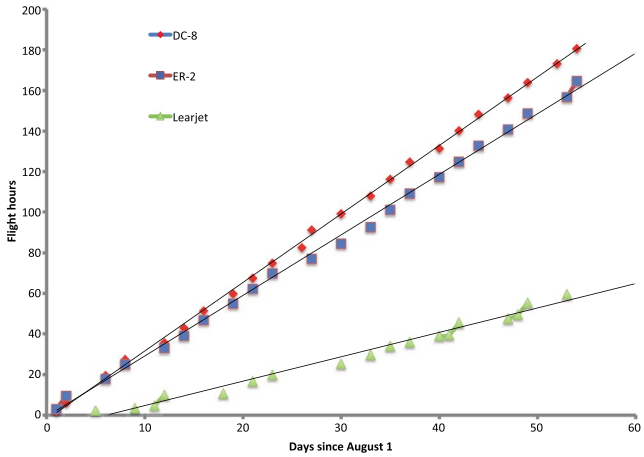

Figure 16. Cumulative flight hours versus time during SEAC4RS. Over 54 days in the field the DC-8 flew 180.6 flight hours, the ER-2 flew 164.6 flight hours, and the SPEC Inc. Learjet flew 59.5 flight hours. The DC-8 made three test flights and 21 science flights. The ER-2 made 1 test flight and 21 science flights. The Learjet made 15 science flights out of 37 total (including test flights, ferry flights, and transits to science flights).

Figure 17 illustrates the flight paths taken by the aircraft during SEAC^{4}RS. Flights covered a large fraction of the U.S., Southern Canada, and the Gulf of Mexico. The majority of flights were aimed at the Southeastern U.S. with the goal of better understanding the chemistry in that region. However, numerous flights occurred over the Western U.S., primarily to sample the plumes from forest fires. Many flights over the Gulf of Mexico were aimed at understanding the role of marine convection or tropical storms in vertical transport. A number of long-range flights were also made to better understand the structure of the lower stratosphere. Figure 6 presents flight dates and times of smoke observations. Flight reports for individual flights may be found at https://espo.nasa.gov/home/seac4rs/mission-flight-docs.

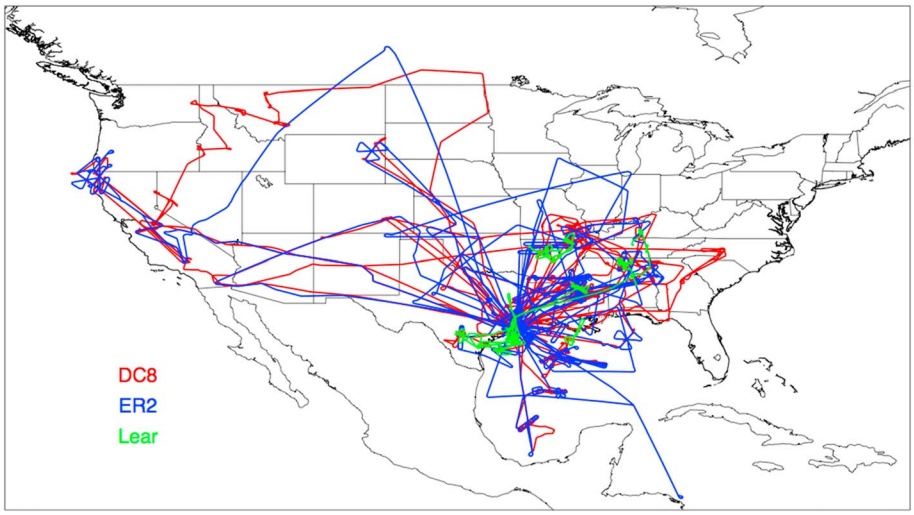

Figure 17. The flight paths taken by the three aircraft during science flights in SEAC^{4}RS.

4.2. Ground Stations, Balloon Flights, and Satellite Retrievals

SEAC^{4}RS established the SouthEast American Consortium for Intensive Ozonesonde Network Study, SEACIONS, an ozonesonde network spread across the U.S. DISCOVER-AQ also sponsored balloon launches from Houston during the SEAC^{4}RS period of operations. A map of the SEACIONS launch sites is given in Figure 18. In total, 222 ozonesondes were launched during the SEAC4RS period. The general goal of SEACIONS was to determine convective impacts on tropospheric ozone and to study gravity waves in the tropical tropopause transition layer. In addition to ozone profiles, water vapor sondes were launched from Ellington Field. In total, 19 water vapor sondes were launched during the SEAC^{4}RS period.

SEAC^{4}RS also set up several AERONET sites to augment the already extensive network in the U.S. AERONET maintains a large global network of Sun-sky photometers, with many sites in the U.S. Northeast. However, there historically have been very few sites in the Southeast United States, with only intermittent data from Huntsville, AL. For SEAC^{4}RS an additional 14 sites were deployed. Favored locations included Interagency Monitoring of Protected Visual Environments (IMPROVE), SEARCH, and EPA air quality sites. An additional mesonet of AERONET Sun photometers was deployed in Houston jointly with the coincident DISCOVER-AQ mission. Figure 4 illustrates the AERONET sites in use during the SEAC^{4}RS operational period for those sites with more than a week of data. In Figure 4 AOTs were interpolated to the MODIS AOT 550 nm wavelength. In this figure it is noteworthy that there are, at times, significant differences between optical thickness at individual AERONET sites and those retrieved by MODIS. This difference is in part due to different sampling. Nevertheless, the patterns of seasonal behavior are consistent between AERONET and MODIS.

Figure 18. The locations of SEACIONS balloon launching facilities used during SEAC^{4}RS. Coordinates at http://croc.gsfc.nasa.gov/seacions.

One SEAC^{4}RS ground site warranted special attention. SEAC^{4}RS took advantage of the University of Alabama at Huntsville facilities that already exist, most notably its Ozone Differential Absorption Lidar (DIAL). The lidar lab was installed with the University of Wisconsin High Spectral Resolution Lidar (HSRL), providing vertical profiles of aerosol backscattering and extinction at 532 nm. The site was also a member of the SEACIONS ozonesonde network, providing daily early afternoon thermodynamic and ozone soundings.

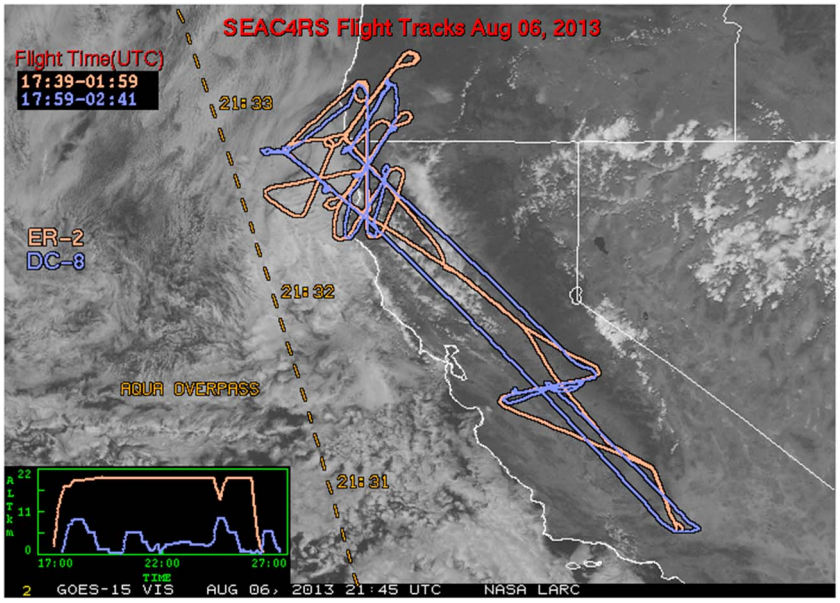

Figure 19. Flight paths for the ER-2 and DC-8 on 6 August 2013. The inset to the figure shows the pressure altitudes of the aircraft versus universal time. The figure background, as noted in the banner at the bottom of the figure, is a GOES 15 image taken at the time and wavelength noted in the banner. Images of flight segments for various times and for both visible and infrared wavelengths can be obtained under the SEAC^{4}RS heading at http://www-pm.larc.nasa.gov. GOES flight track overlay figures courtesy of Doug Spangenberg.

SEAC^{4}RS also collaborated with the mobile and fixed research radars in Huntsville, Alabama. SEAC4RS data are complementary to data from many of the numerous atmospheric chemistry measurement sites across the U.S. including the IMPROVE network, the SEARCH network, EPA sites, and state air quality networks.

Imagery from 4 km GOES east and GOES west taken at high temporal resolutions was analyzed to retrieve cloud properties and top-of-atmosphere (TOA) radiative fluxes during all SEAC^{4}RS flights. Cloud phase, heights, optical thicknesses, and effective particle sizes as well as other parameters were retrieved using

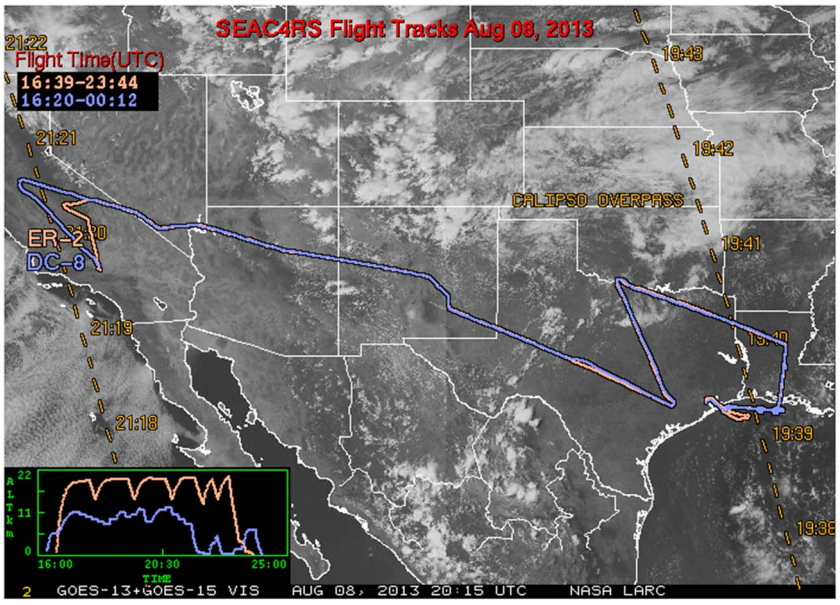

Figure 20. Flight tracks of the DC-8 and ER-2 on 8 August 2013. Details of Figure 20 are noted in the caption to Figure 19. In Figure 20, GOES 13 data are used as noted in the banner at the bottom of the figure.

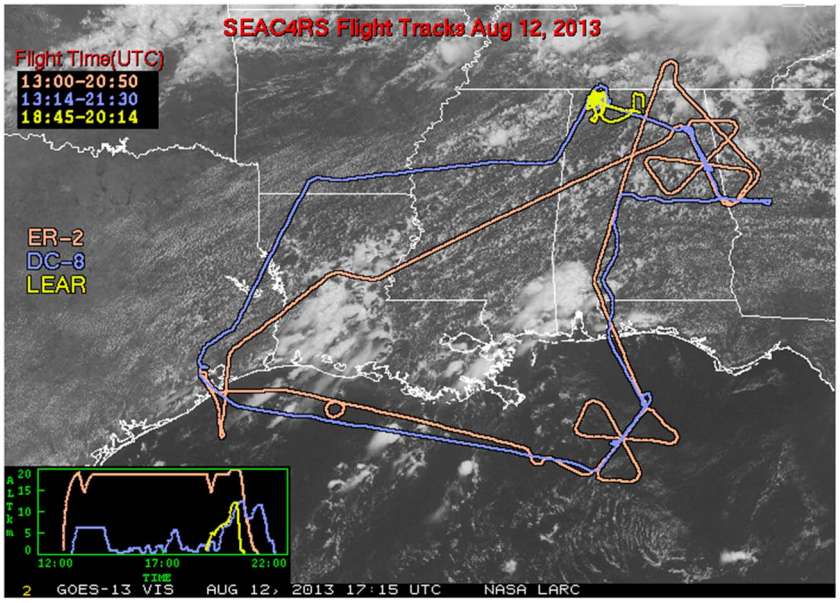

Figure 21. The flight tracks of the ER-2, DC-8, and Learjet are shown for 12 August 2013. Details of Figure 21 are noted in the caption to Figure 19.

the methods of *Minnis et al*. [2011], while TOA shortwave albedo and outgoing longwave flux were estimated from the GOES visible and 11 μm channels as in *Minnis and Smith* [1998] with the improvements developed by *Khaiyer et al*. [2009]. The occurrences of overshooting tops, i.e., penetrations of convective clouds into the stratosphere, were determined for each image using the technique of *Bedka et al*. [2010]. The flight tracks for each aircraft are overlaid on each relevant GOES visible and infrared image to provide context for each flight (see examples in Figures 19–41). Summary flight track overlays were also produced for each flight centered on the visible and infrared images corresponding to the middle of the flight. In addition to the full domain retrievals for each image, the retrieved properties were matched and averaged along the flight tracks and the Huntsville, Alabama site. The images are available at http://www-pm.larc.nasa.gov/SEAC4RS.

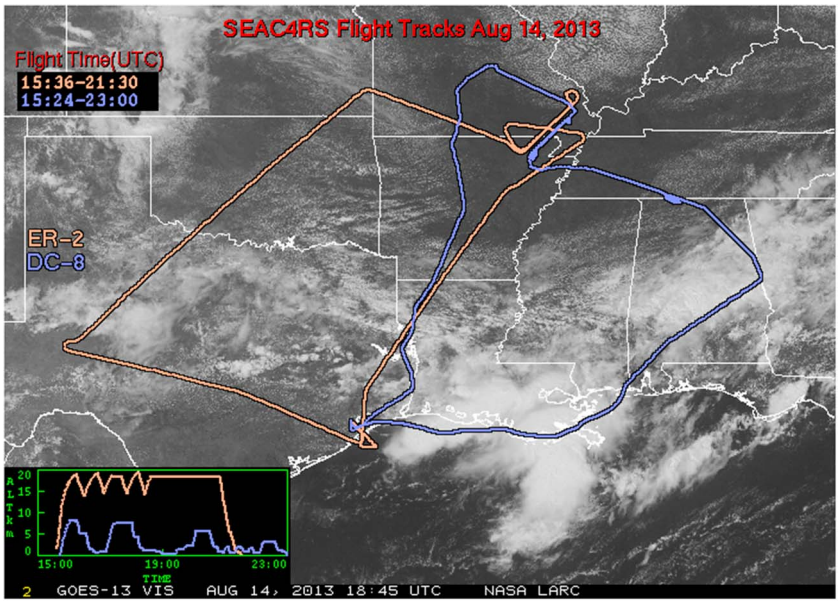

Figure 22. The flight tracks of the ER-2 and DC-8 are shown for 14 August 2013. Details of Figure 22 are noted in the caption to Figure 19.

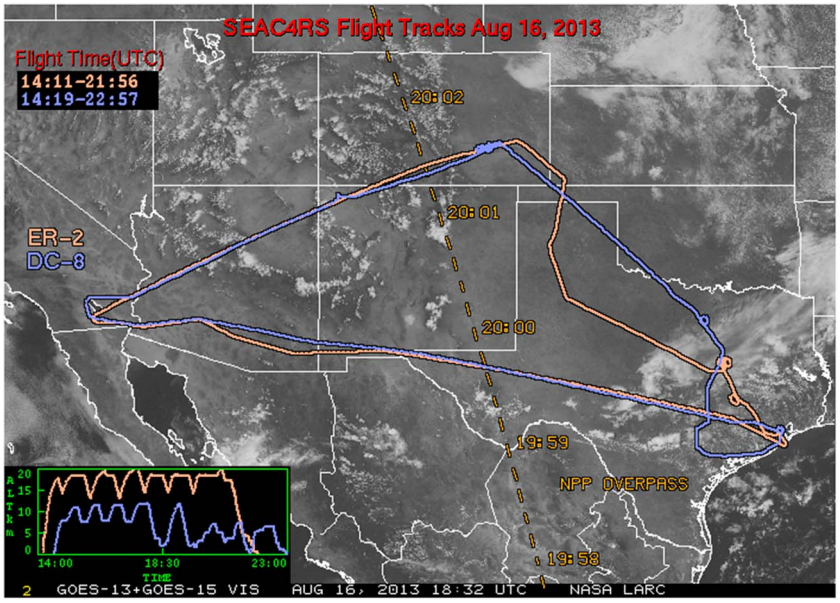

Figure 23. The flight tracks of the ER-2 and DC-8 are shown for 16 August 2013. Details of Figure 23 are noted in the caption to Figure 19.

4.3. Goals and Highlights of Individual Flights

Table 3 describes the goals for each of the 23 science flight days during SEAC^{4}RS. This section provides an overview of each of the flights with the aid of summary flight tracks overlaid on GOES visible images for each flight. Most flights achieved multiple goals as can be noted by the density of points in Table 3. Test flights and flights to reposition the aircraft are not described unless they were part of a science related mission. The goal of the descriptions below is to aid investigators looking for data about specific science questions in determining the data sets that are most relevant and to put the data from the separate aircraft into the context of the data from the other aircraft.

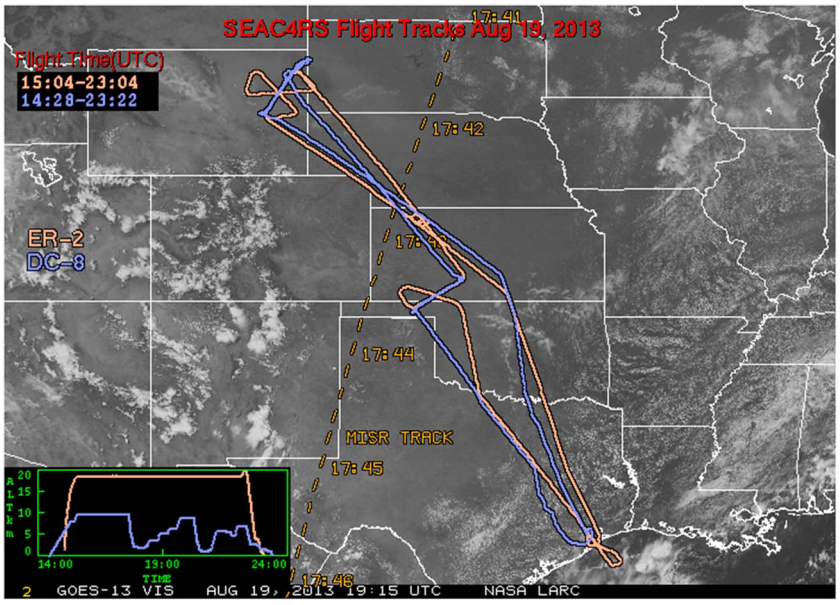

Figure 24. The flight tracks of the ER-2 and DC-8 are shown for 19 August 2013. Details of Figure 24 are noted in the caption to Figure 19.

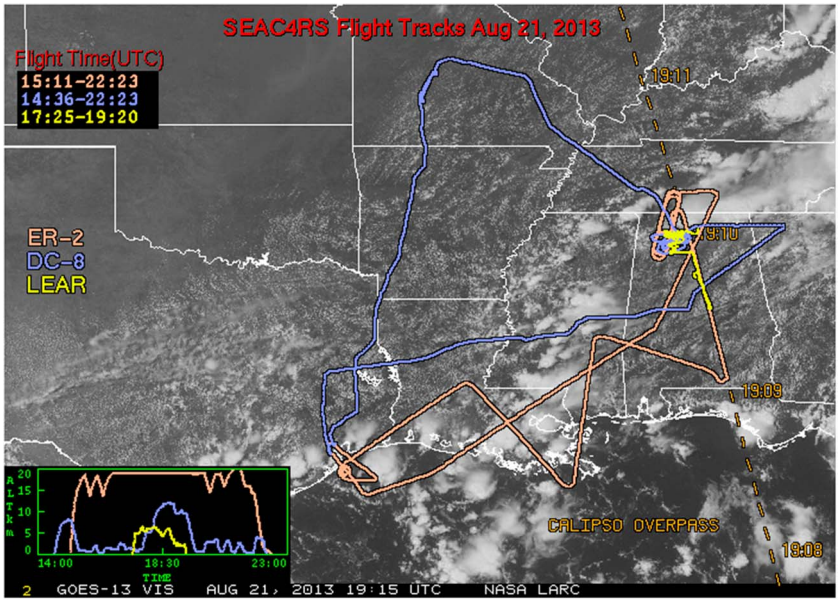

Figure 25. The flight tracks of the Learjet, ER-2, and DC-8 are shown for 21 August 2013. Details of Figure 25 are noted in the caption to Figure 19.

4.3.1. The 6 August 2013 Flight

The primary goal of this flight was to obtain coordinated MODIS, ER-2 and DC-8 measurements of smoke above clouds off the west coast. The flight tracks are shown in Figure 19. The flight succeeded in acquiring remote sensing measurements from the ER-2 simultaneous with in situ and remote measurements from the DC-8 of smoke both over the land and over marine stratus. The aircraft were well coordinated for these measurements particularly over the ocean. Flying through smoke over the land is more challenging due to the mountainous terrain. Smoke over stratus is of interest and the concurrent MODIS overpass has already been used to develop an experimental retrieval for MODIS to measure aerosols in cloudy areas. Smoke was thick enough to obscure the ground. A CALIPSO overpass occurred near 21:30 off the Oregon coast.

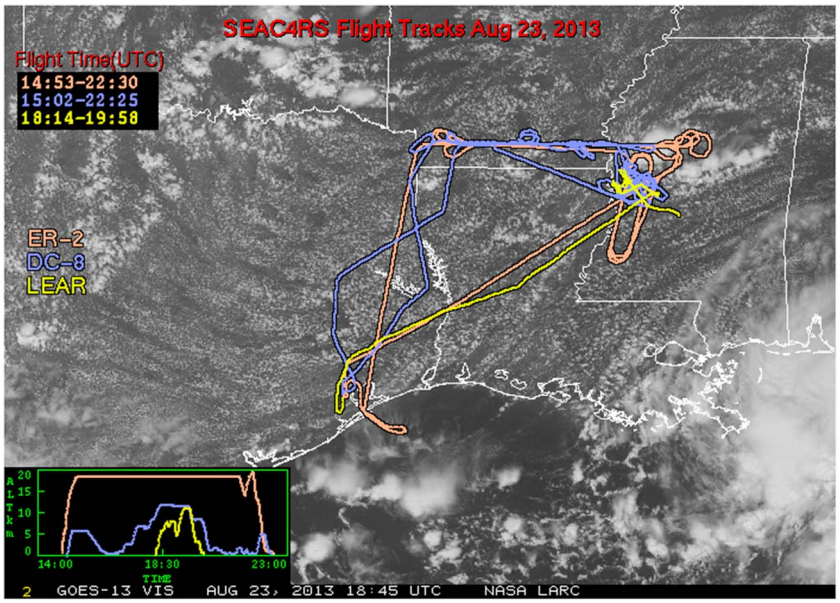

Figure 26. The flight tracks of the Learjet, ER-2, and DC-8 are shown for 23 August 2013. Details of Figure 26 are noted in the caption to Figure 19.

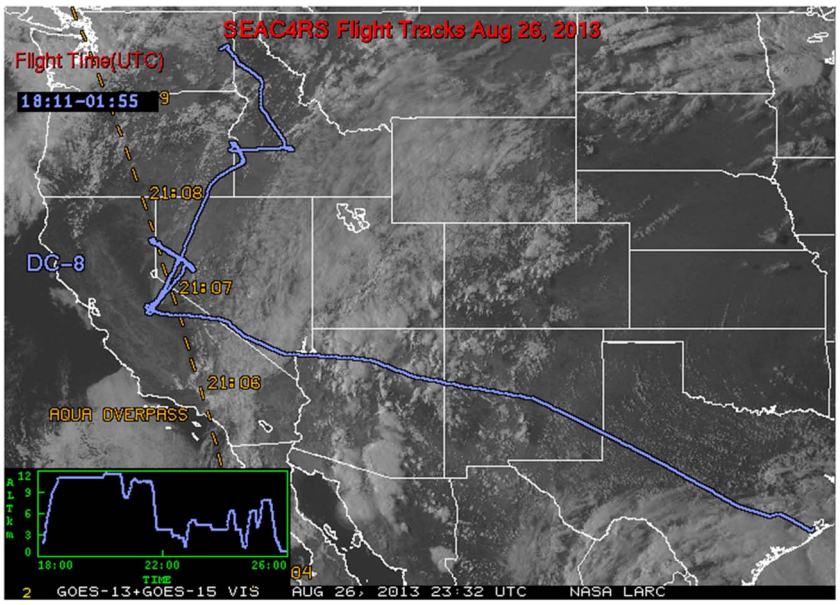

Figure 27. The flight track of the DC-8 is shown for 26 August 2013. Details of Figure 27 are noted in the caption to Figure 19.

Coincident airborne HSRL measurements of smoke over the marine stratus clouds have been used to validate CALIOP retrievals of smoke optical thickness that utilize backscatter and depolarization measurements of the stratus clouds. Both aircraft also performed measurements over the Central California valley, with the DC-8 making vertical profiles near Fresno, CA, while the ER-2 made remote sensing observations above the DC-8.

4.3.2. The 8 August 2013 Flight

This flight, during which the ER-2 and DC-8 transited from NASA's Armstrong Flight Research Center in California to Ellington Field near Houston, Texas, was aimed at profiling the North American Monsoon, and sampling a layer of Saharan dust over Texas, Southern Louisiana, and the Gulf of Mexico south of Houston. The DC-8 and ER-2 flights were planned to have "stacked" sampling with the ER-2 profiling vertically around the tropopause level and DC-8 sampling the lower boundary level of the monsoonal circulation. Both aircraft

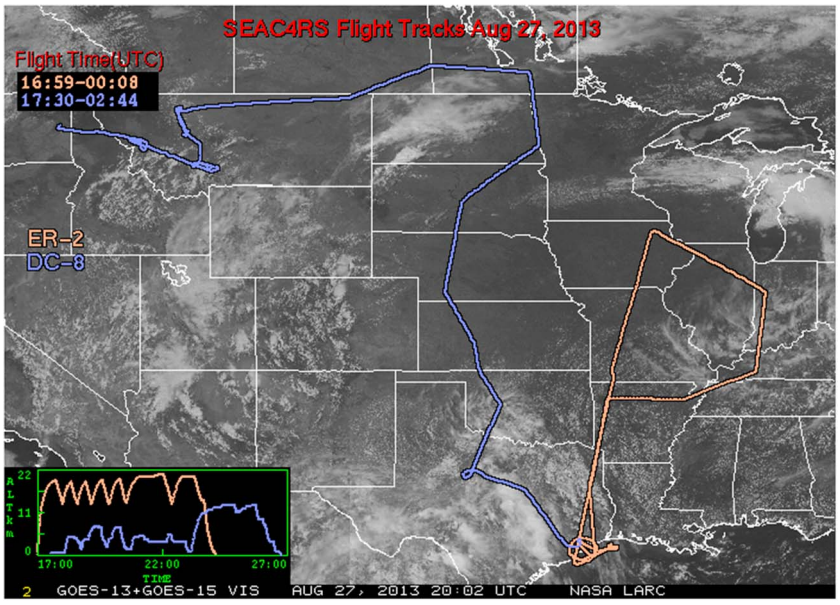

Figure 28. The flight tracks of the DC-8 and the ER-2 are shown for 27 August 2013. Details of Figure 28 are noted in the caption to Figure 19.

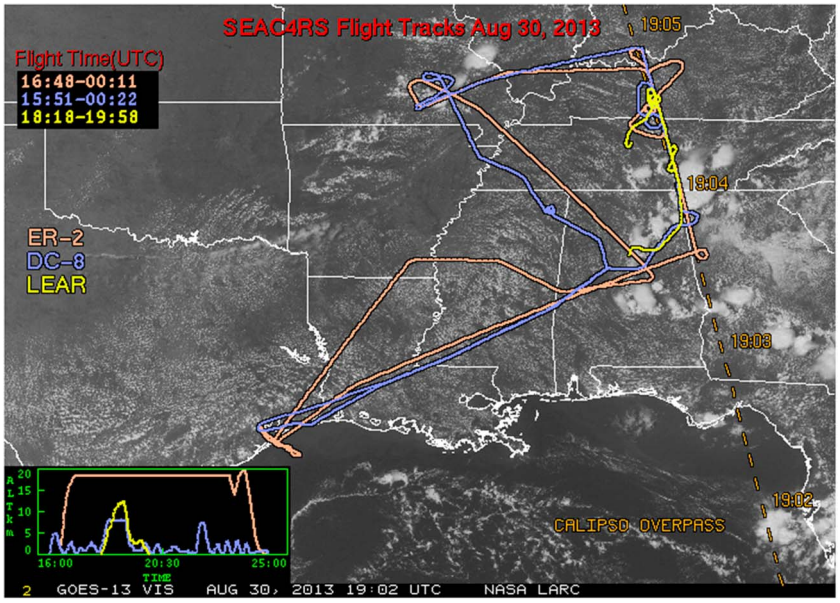

Figure 29. The flight tracks of the Learjet, DC-8, and ER-2 are shown for 30 August 2013. Details of Figure 29 are noted in the caption to Figure 19. Note the CALIPSO overpass track on Eastern boundary of study region.

sampled large air mass gradients crossing the jet stream near 34°N latitude. Both the ER-2 and the DC-8 sampled the lower stratosphere north of the jet core and the upper troposphere south of the jet. The aircraft were tightly coordinated in time during the dust plume measurements over the Gulf of Mexico. The flight tracks are illustrated in Figure 20. Numerous vertical profiles were conducted to investigate the tracer fields, which showed interesting layers of enhanced water vapor above the local tropopause mostly near and over Texas.

4.3.3. The 12 August 2013 Flight

All three aircraft investigated biogenic emissions over the Southeastern U.S., their interactions with urban pollutants, radiative properties of aerosols, and transport to the UTLS in a convective environment. The DC-8 performed a number of vertical profiles below the ER-2 for radiation measurements over the relatively

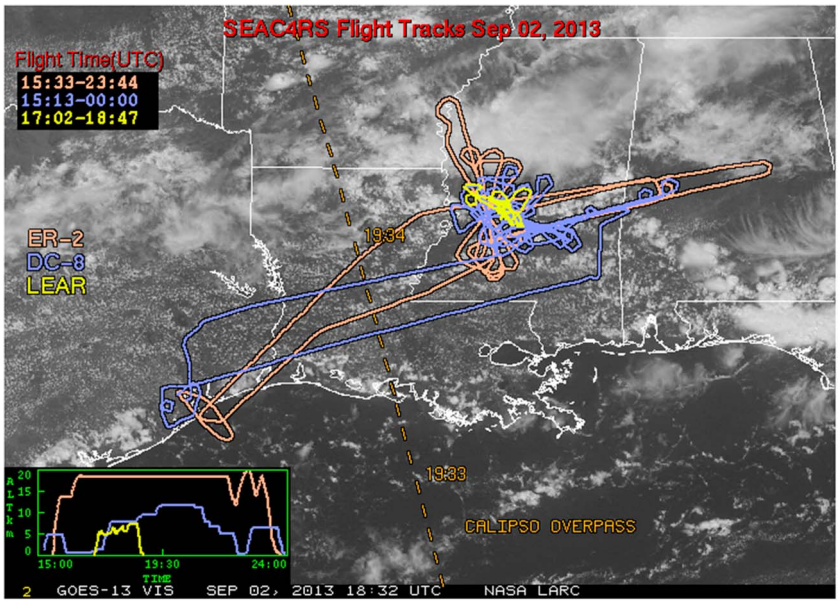

Figure 30. The flight tracks of the Learjet, DC-8, and ER-2 are shown for 2 September 2013. Details of Figure 30 are noted in the caption to Figure 19.

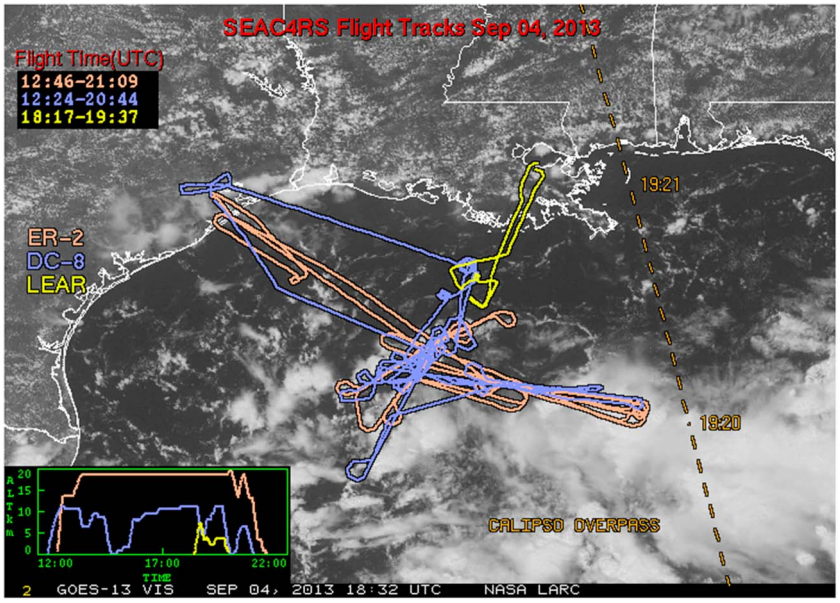

Figure 31. The flight tracks of the Learjet, DC-8, and ER-2 are shown for 4 September 2013. Details of Figure 31 are noted in the caption to Figure 19.

clean marine atmosphere and then over the relatively polluted Southeastern region near Birmingham, Alabama. ER-2 maneuvers for radiative measurements are shown as the two "three-leaf clovers" or rosettes in Figure 21. Cirrus clouds were present during much of the time spent on the rosette near Birmingham. Following the radiation measurements near Birmingham, the ER-2 returned to Ellington Field, while the DC-8 and the Learjet rendezvoused near Muscle Shoals, Alabama. They then chose a convective cell to sample from near its base to cloud top. The maneuvers around the convection are shown as the small "knot" in Northern Alabama in Figure 21 and by the DC-8 climb to cloud top altitudes near 11 km in the altitude profile in the inset in Figure 21. During the convective cloud sampling the Advanced Radar for Meteorological and Observational Research (ARMOR) dual-polarization radar at Huntsville was able to observe the clouds

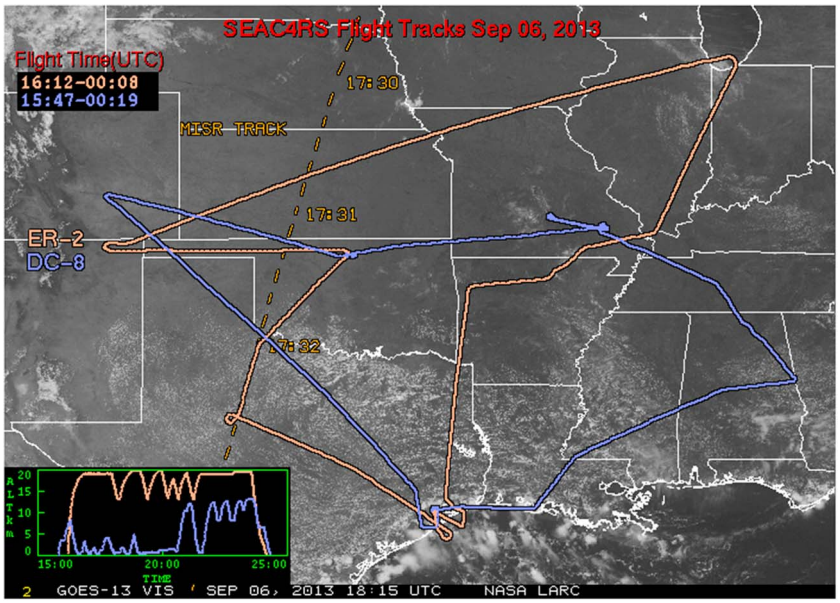

Figure 32. The flight tracks of the DC-8 and ER-2 are shown for 6 September 2013. Details of Figure 32 are noted in the caption to Figure 19.

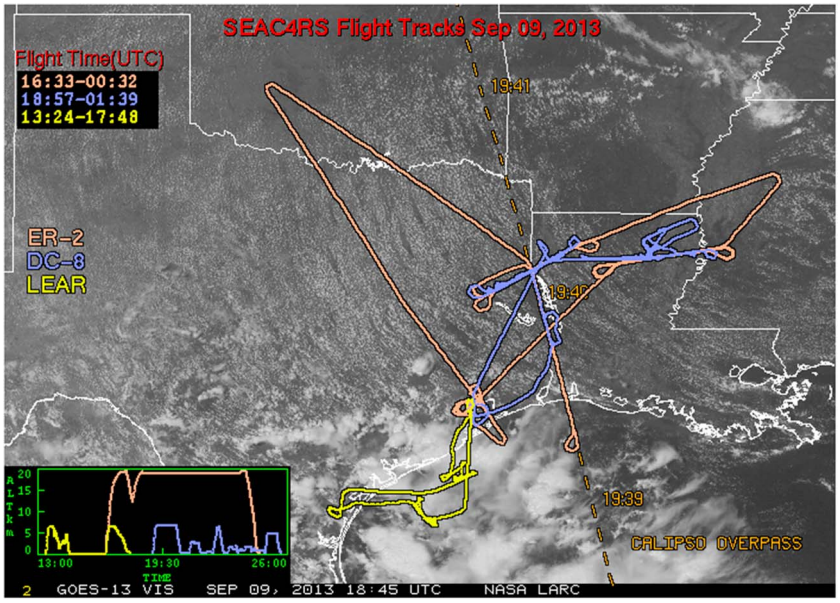

Figure 33. The flight tracks of the DC-8 and ER-2 are shown for 9 September 2013. Details of Figure 33 are noted in the caption to Figure 19.

being sampled by the DC-8 and the Learjet. Sampling showed isoprene and its oxidation products above cloud top, as well as in the boundary layer demonstrating vertical transport and associated chemistry. During the flights AERONET sites at Pensacola, Florida; Centreville, Alabama; and Huntsville, Alabama were overflown.

4.3.4. The 14 August 2013 Flight

On this day the DC-8 and ER-2 flew missions with partially independent goals. As illustrated in Figure 22 the DC-8 first flew along the coast of Louisiana to sample marine boundary layer air. It turned north near the border between Alabama and Mississippi, but had to ascend to get through a line of convection. The aircraft was able to move into the boundary layer west of Atlanta, and then performed a series of short legs at different levels near the Mingo, Missouri, AERONET site. Meanwhile the ER-2 flew across Texas, Oklahoma,

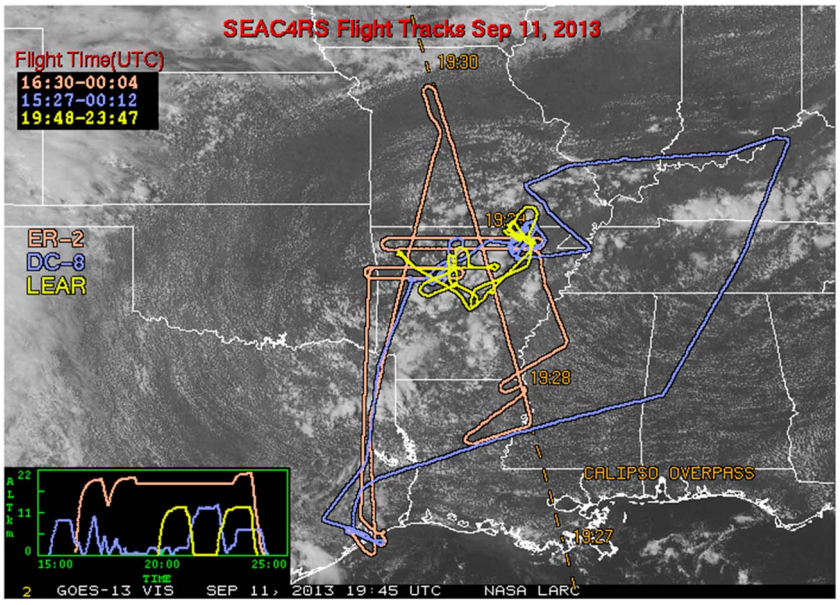

Figure 34. The flight tracks of the DC-8 and ER-2 are shown for 11 September 2013. Details of Figure 34 are noted in the caption to Figure 19.

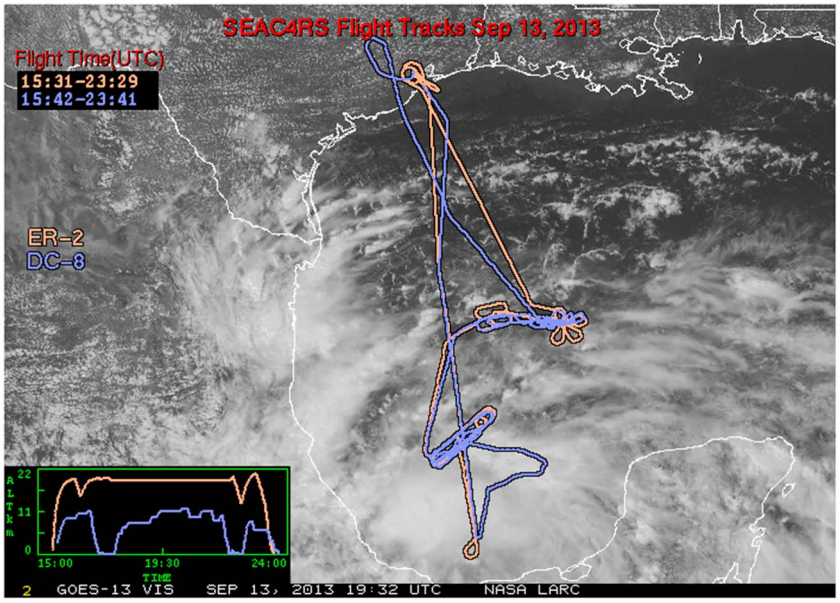

Figure 35. The flight tracks of the DC-8 and ER-2 are shown for 13 September 2013. Details of Figure 35 are noted in the caption to Figure 19.

and Kansas, performing vertical profiles to sample a gradient across the North American Monsoon. One profile over Central Texas occurred above a decaying MCC. The ER-2 then proceeded to the Mingo, Missouri, AERONET site where it performed part of a rosette pattern above the DC-8. During this phase of the flight both aircraft encountered smoke that had been forecast to be present from fires in Idaho. The ER-2 had to cut short its radiation measurements, dropping legs from the rosette, due to bad weather closing in at Ellington Field. The DC-8 sampled air over the Ozarks in Arkansas and over Louisiana during its return to Ellington Field.

4.3.5. The 16 August 2013 Flight

On this flight the DC-8 and ER-2 first flew to California performing a series of vertical profiles in order to probe the North American Monsoon as illustrated in Figure 23. En route, the ER-2 encountered the remnants of

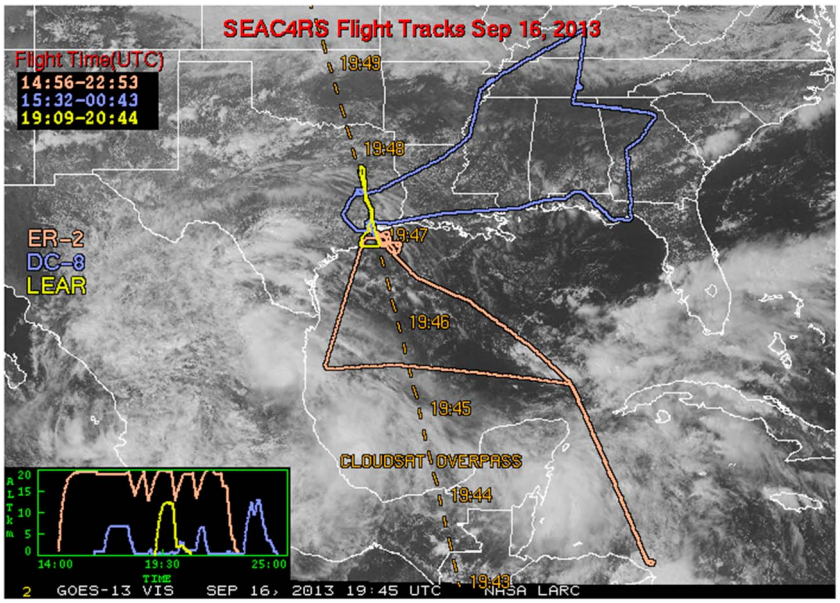

Figure 36. The flight tracks of the Learjet, DC-8, and ER-2 are shown for 16 September 2013. Details of Figure 36 are noted in the caption to Figure 19.

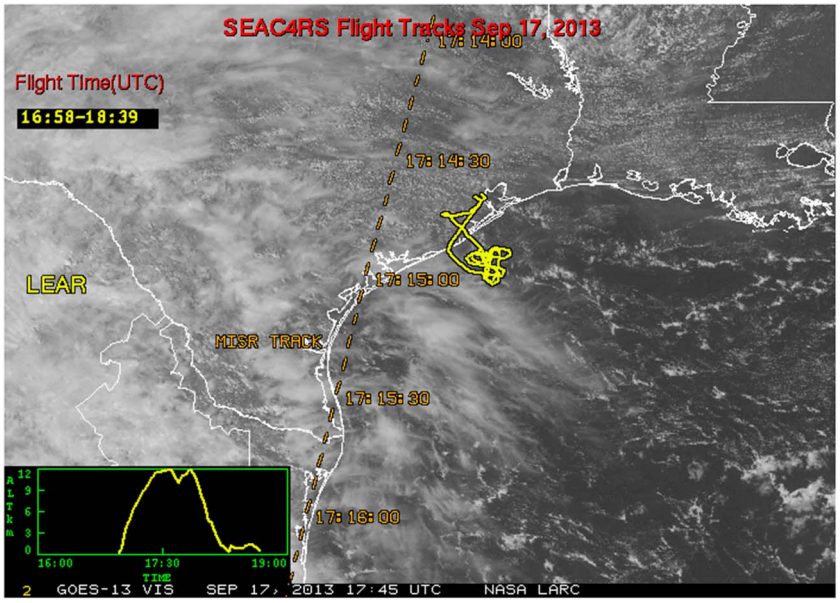

Figure 37. Learjet flight on 17 September 2013. Details of Figure 37 are noted in the caption to Figure 19.

an MCC near Houston. From California, the DC-8 flew through the plume of the Four Corners power plant. Both aircraft then proceeded east of the Rocky Mountains where they flew several legs to characterize an aged smoke plume with a visible wavelength optical thickness on the order of 0.4 that had advected to Colorado from Idaho. On the return to Ellington, the DC-8 performed a missed approach at an airport near Dallas to characterize its urban plume and to characterize CH_4 and VOCs in a region possibly impacted by emissions from gas and oil extraction activities in the Barnett Shale. The ER-2 flew an underpass of the NPP satellite at about 20:00 UT over Central Texas.

4.3.6. The 19 August 2013 Flight

The principal goal of this joint ER-2, DC-8 flight, illustrated in Figure 24, was to target aged smoke from fires in Wyoming and Idaho. The DC-8 transited to Wyoming at an altitude of about 30 kft. En route, the aircraft

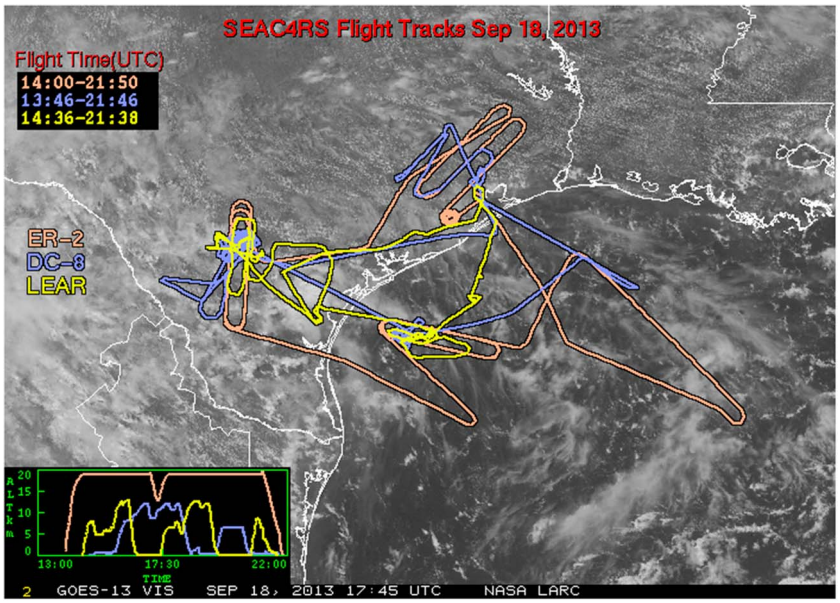

Figure 38. The flight tracks of the Learjet, DC-8, and ER-2 are shown for 18 September 2013. Details of Figure 38 are noted in the caption to Figure 19.

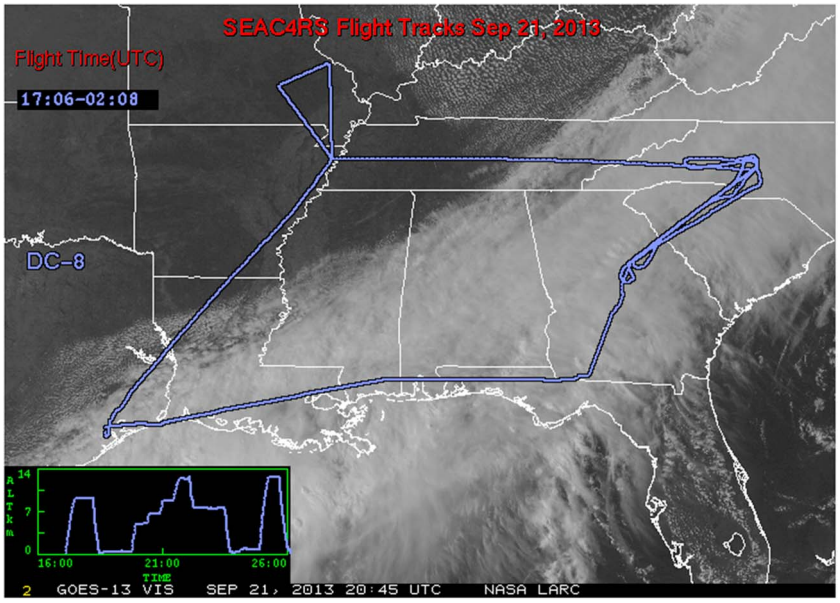

Figure 39. The flight tracks of the Learjet, DC-8, and ER-2 are shown for 21 September 2013. Details of Figure 39 are noted in the caption to Figure 19.

encountered cirrus shortly after takeoff, and then high levels of NO_x over Northern Texas and Southern Oklahoma, which may have come from convection in Colorado the night before. The DC-8 observed layers of smoke essentially all the way between the Southern Great Plains CART site in Northern Oklahoma, and Wyoming. Some of these smoke layers had optical thicknesses of almost 0.8. At the northern end of the flight track the DC-8 flew a series of legs at various altitudes to profile the smoke, while the ER-2 flew a rosette pattern overhead to make polarimetric observations of the smoke. Both aircraft then flew to the Oklahoma-Kansas border where they performed a second set of vertical profiles and radiation legs for the polarimeters to examine somewhat older smoke. During this time there was an overpass of the MISR instrument on the Terra satellite. An excellent satellite to in situ intercomparison opportunity in smoky conditions was obtained.

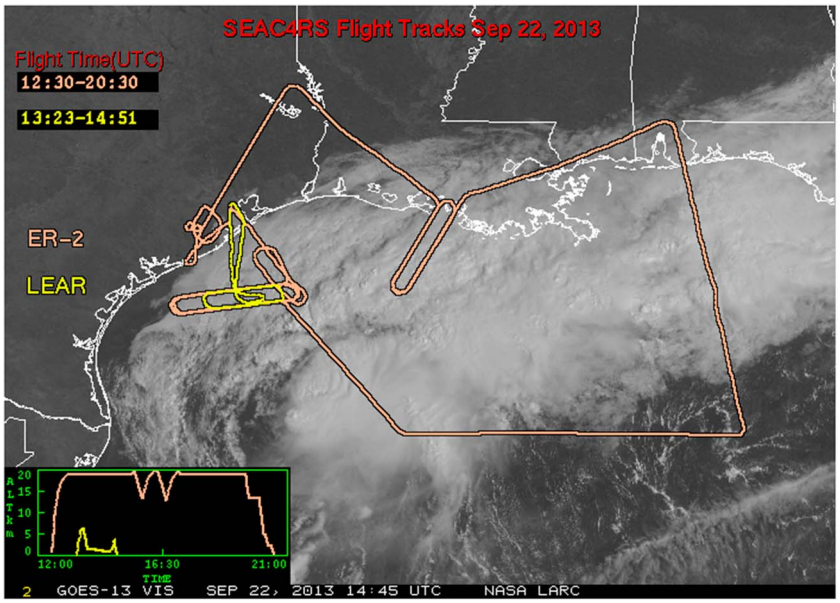

Figure 40. The flight tracks of the Learjet and ER-2 are shown for 22 September 2013. Details of Figure 40 are noted in the caption to Figure 19.

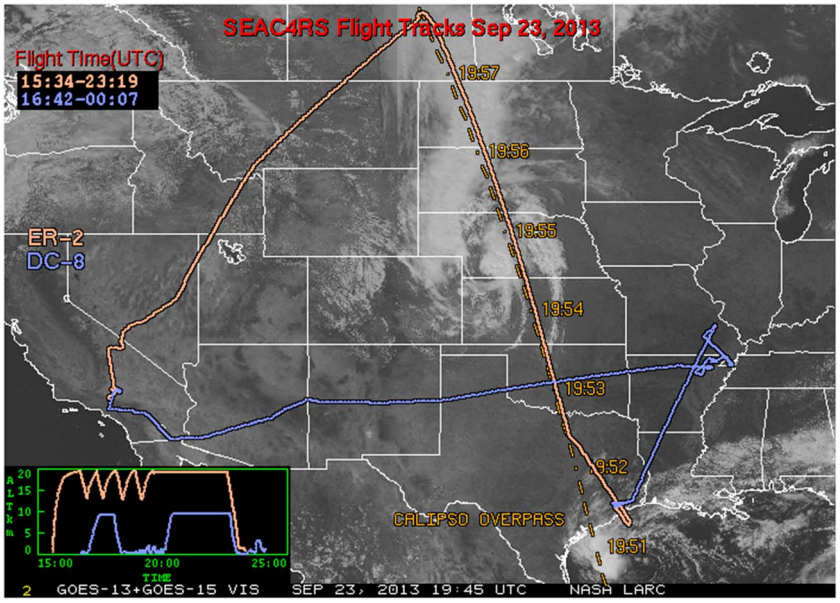

Figure 41. The flight tracks of the DC-8 and ER-2 are shown for 23 September 2013. Details of Figure 41 are noted in the caption to Figure 19.

The DC-8 observed smoke most of the way back to Houston, with some mixing into the boundary layer near Houston. On landing in Houston the DC-8 did several legs in the boundary layer, including one in the Houston ship channel.

4.3.7. The 21 August 2013 Flight

This flight mission involved all three aircraft, as well as research radars at Huntsville, Alabama. The goal of the DC-8 was to sample biogenic emissions and chemistry over the Southeastern U.S. and to examine vertical transport in a convective environment. As illustrated in Figure 25, the DC-8 first flew northeast and then made boundary layer observations near Centreville, Alabama, which is an Impact Program chemistry site. Low clouds hampered flying in the boundary layer at earlier times. The DC-8 then proceeded to Muscle Shoals, AL, where it met up with the Learjet and the ER-2. The ER-2 made a series of oval racetracks above the convective environment which contained mature anvils, while the DC-8 and the Learjet made a series of cloud base, anvil, and above-cloud penetrations. The DC-8 then sampled the upper troposphere searching for convective transport signatures. It then proceeded to the Ozarks where it sampled various biogenic emissions. En route to the convective cloud sampling near Muscle Shoals, the ER-2 conducted a series of vertical profiles over Louisiana and Alabama searching for evidence of recent convective outflow. After leaving the racetrack pattern the ER-2 flew along a CALIPSO track over Alabama in coordination with an overpass. Cirrus was present along this flight leg. The Learjet flew in shallow cumulus along the same track. On the return to Ellington, the ER-2 did a series of vertical profiles over Mississippi to look for convective detrainment at high altitude.

4.3.8. The 23 August 2013 Flight

This flight, involving three aircraft, was aimed at understanding diurnal changes in biogenic emissions mainly in southern Arkansas and convective pumping over Alabama. The DC-8 and ER-2 flew first to southern Arkansas and then flew a series of racetracks in the east-west direction across the state sampling biogenic emissions, as illustrated in Figure 26. They then met the Learjet over Mississippi. The Learjet and DC-8 profiled a convective system from the boundary layer to above the cloud tops, while the ER-2 made remote sensing observations of the clouds from above. The ER-2 and DC-8 then made several more racetrack patterns across southern Arkansas to the Mississippi river. The DC-8 made a deep vertical profile by making a missed approach at Texarkana en route to Ellington Field.

4.3.9. The 26 August 2013 Flight

On this day, the DC-8 flew to California to investigate the smoke plume from the Rim Fire near Yosemite, as illustrated in Figure 27. This fire was the third largest by area in the history of California. The ER-2 planned to investigate the North American Monsoon, but bad weather in Houston caused the flight to be canceled.

The DC-8 profiled along the base of the NAM on its path to California, and did a short leg to do in situ sampling of cirrostratus. The DC-8 profiled the Rim Fire source region from above with DIAL, coincident with an A-Train Aqua overpass and made two wall-type passes through the fresh smoke above the fire. Tall smoke towers and pyrocumulus were observed. The DC-8 then followed the smoke plume northward, making two vertical profiles: first, near Reno, Nevada, followed by a downwind wall near Boise, Idaho. Generally, it was not possible to fly level legs beneath the smoke plume (for the radiation measurements) as the plume was mixed into the boundary layer to the surface. At times along this transect the DC-8 sampled smoke-filled boundary layer clouds. The DC-8 proceeded into Idaho, where other fires were burning. While smoke from the Little Queens fire was sampled briefly, it was concluded that the mountainous terrain would not allow extensive sampling. The aircraft landed in Spokane, Washington, where it spent the night. Along the flight path the aircraft overflew the AERONET site at the University of Nevada in Reno.

4.3.10. The 27 August 2013 Flight

The DC-8 and ER-2 flew independent flights on this day, as illustrated in Figure 28. The DC-8 made a missed approach at Missoula Montana, and executed a wall near Bozeman Montana. Each of these locations is an AERONET site and Bozeman has additional remote sensing ground instruments. A wall was also executed west of Great Falls through smoke and clouds. Numerous profiles were made through smoke and clouds, and two radiation walls were conducted, the second in a region with abundant boundary layer capping cumulus. The smoke was patchy, and some smoke may have been encountered from fires other than the Rim Fire. The DC-8 then flew to Winnipeg Canada, sampling smoke along the entire path with several altitude changes. Along the flight leg from Winnipeg to Ellington Field, the DC-8 flew between 34 and 40 kft, profiling the upper troposphere. Near Ellington a layer of cirrus was sampled; several boundary layer tracers were enhanced in and near the cirrus clouds. Together the 26 and 27 August flights represent the longest research flights ever made in aging smoke from a single fire. The goal of the ER-2 flight on 27 August was to sample the impact of the NAM on the UTLS with a series of vertical profiles. A layer of significantly enhanced water vapor above the tropopause was evident in three vertical profiles south of the Great Lakes, downstream from a large migrating MCC. AERONET sites at Bondville, Illinois; St. Louis, Missouri; Mingo, Missouri; and Upper Buffalo, Arkansas were targeted for comparison with remote sensing measurements of aerosols.

4.3.11. The 30 August 2013 Flight

On this day all three aircraft were used, as illustrated in Figure 29. The DC-8 sampled gas phase and aerosol chemistry in hot and humid conditions over the Southeastern U.S. The DC-8 first flew in the boundary layer from Louisiana to Birmingham, Alabama with multiple profiles from 1–2 kft to above the tops of fair weather cumulus near 6 kft. Near the Alabama/Georgia border the DC-8 turned down the track of CALIPSO and flew under a layer of cirrus until the point of the CALIPSO overpass near the Mammoth Caves AERONET site in Kentucky, where it met the ER-2 and Learjet. There the aircraft made a vertical profile with 4 min legs at 1, 5, and 25 kft. The DC-8 then proceeded to do further boundary layer profiles to Missouri, where the aircraft was able to enter restricted air space not far from the Mingo AERONET site in a region with very high levels of isoprene, low NO_x, and low formaldehyde. The DC-8 was able to make boundary layer measurements back to Georgia, and on the return to Ellington sampled the industrial areas of Port Arthur and Beaumont, Texas. The ER-2 flew over three AERONET sites: Centreville, Alabama; Mammoth Caves, Kentucky; and Leland High School, Mississippi. These observations should help evaluate optical thickness retrievals from the polarimeters on the ER-2. The ER-2 and the Learjet both flew along the CALIPSO track. The Learjet sampled cirrus along this route.

4.3.12. The 2 September 2013 Flight

The three aircraft flew a coordinated flight to characterize the lifecycle of continental convection as illustrated in Figure 30. The three aircraft met just west of Jackson, Mississippi. The DC-8 characterized the boundary layer before the onset of convection. Once convection began, the DC-8 made a series of passes through the turrets, as did the Learjet. After identifying a particularly robust cell, the DC-8 and Learjet profiled the cell with the DC-8 sampling outflow from the clouds. The DC-8 then joined up with the ER-2 and made a series of long racetracks trying to characterize the cloud field that the ER-2 was observing remotely. Afterward, the DC-8 sampled air near the freezing level, small cumulus, and the boundary layer before eventually exiting the convective region. The ER-2 made several vertical profiles near the end of the flight to characterize cirrus clouds in the upper troposphere. A CALIPSO overpass occurred near 1900 UT.

4.3.13. The 4 September 2013 Flight

This flight was parallel to the flight on 2 September 2014, except that maritime convection was targeted as shown in Figure 31. In addition, the Learjet and the ER-2 collected data along an overpass track of the A train.

The DC-8 first flew in outflow cirrus and a series of turrets. It then underflew the ER-2 as it made several patterns for cloud radiation measurements. At the conclusion of these radiation measurements, the DC-8 descended into the boundary layer and characterized it while the ER-2 flew lines above the cloud field. The DC-8 then penetrated a number of convective turrets at different levels, while the ER-2 made radiative observations in the same area. The Learjet also penetrated many of these turrets.

4.3.14. The 6 September 2013 Flight

This mission involved the ER-2 and the DC-8 flying over the Southern U.S. as shown in Figure 32. The ER-2 obtained polarimeter data along a flight track of the MISR instrument on the AURA satellite, vertical profiles over the DOE Southern Great Plains ARM site and in the North American Monsoon, and overflew AERONET sites at Mingo, MO, and Upper Buffalo, AR (where skies were partly cloudy), to evaluate polarimeter retrievals of aerosols. The DC-8 surveyed boundary layer chemistry in the Southeastern U.S., particularly over an oak forest in western Tennessee, and conducted an isoprene flux experiment over SE Missouri, by flying at multiple levels. Interesting gradients in NO_x were found along these flight legs. After leaving the Ozarks the DC-8 complemented the ER-2 vertical profile over the DOE ARM site to validate TCCON measurements and sampled the decaying NAM over Southern Colorado. The DC-8 encountered aged smoke layers that may have come from fires in California, over the track from Alabama to Missouri, and sampled smoke from an agricultural fire in the Mississippi Valley. Interesting gradients in NO_x were found along these flight legs. On the return to Houston the DC-8 conducted a lidar profile over Houston, to support the NASA DISCOVER-AQ mission, which was also flying out of Ellington Air Field.

4.3.15. The 9 September 2013 Flight

This mission involved the ER-2 and the DC-8 flying over the Southeastern U.S. as shown in Figure 33. The DC-8 targeted northern Louisiana, to sample emissions from oil and gas extraction in the Haynesville Shale; terpenes, and isoprene from a region thought to be a strong source of terpenes; and two agricultural fires in the Mississippi River valley. The DC-8 flew an underpass of CALIPSO along the border between Texas and Louisiana. This underpass, coordinated with the ER-2, also passed over a mobile AERONET site 3 times. The DC-8 and ER-2 flew similar coordinated patterns over a second mobile AERONET site at the eastern end of the target region. A pyrocumulus was noted by the ER-2 and DC-8 pilots but dissipated before it could be sampled. The DC-8 penetrated a smoke plume from an agricultural fire multiple times. On the return to Houston, the DC-8 conducted a missed approach at the Shreveport airport in order to get closer to the surface in a region with extensive oil and gas extraction. The ER-2 also performed several vertical profiles over Southern Oklahoma, to examine stratospheric water vapor and ozone.

4.3.16. The 11 September 2013 Flight

On this day all three aircraft made a coordinated flight to examine convection over Arkansas, as indicated in Figure 34. The ER-2 first did a vertical profile to sample lower stratospheric chemistry on the way to Missouri, where it turned southeast and flew along a CALIPSO satellite track. The ER-2 then overflew mobile AERONET sites at Baskin, LA, and Leland, MS. The ER-2 then flew east-west racetracks above a field of convective clouds that were intensively sampled by the DC-8 and Learjet. The hope was that there would be a large gradient in smoke along the track that would be reflected in the cumulus clouds along the track. However, it appeared that the smoke was more uniform than hoped on the basis of the optical thicknesses of aerosol at the Upper Buffalo, AR, and Leland, MS, AERONET sites. The DC-8 initially flew to Kentucky, and then down the Ohio River Valley. The valley air contained organic aerosols that were more abundant than sulfates and had a total aerosol optical thickness near 0.4. Over the Ozarks there were high concentrations of isoprene and considerable urban pollution and smoke from fires so that visibility was limited. The DC-8 sampled an agricultural fire from source to downwind, observing rapid O_3 and PAN formation. Next, the DC-8 and Learjet sampled cumulus. The DC-8 sampled inflow air, then climbed to about 41 kft, and extensively sampled outflow. The DC-8 then sampled another convective system from top to bottom and was joined by the Learjet and the ER-2. High levels of isoprene and CO, and both high and low NO_x environments were encountered in the outflow. At the end of the flight, the DC-8 made an east-to-west pass over Houston profiling ozone to support the DISCOVER-AQ program.

4.3.17. The 13 September 2013 Flight

The goal of this set of flights was for the ER-2 and DC-8 to observe the cirrus above tropical storm Ingrid, and then to sample marine convective clouds. En route to Ingrid, located in the Bay of Campeche near the coast of the Yucatan, the ER-2 performed a vertical dip to profile the chemistry in the lower stratosphere and upper troposphere (Figure 35). While the ER-2 sampled the air above Ingrid, the DC-8 descended into the boundary

layer and measured the chemistry impacted by oil and gas extraction over the water near the Yucatan for 30–40 min. The DC-8 and ER-2 then did a racetrack pattern to characterize the local cirrus field. Both aircraft then proceeded about halfway back to Houston, where the ER-2 did a series of rosette patterns over a set of convective cells that were profiled by the DC-8. The ER-2 descended over Houston to profile ozone, while the DC-8 did a DIAL lidar cross section to support DISCOVER-AQ.

4.3.18. The 16 September 2013 Flight

On this day, the three aircraft flew separate patterns as shown in Figure 36. The ER-2 flew south through the Yucatan straits with the goal of sampling stratospheric air chemistry as far south as possible. On the return the ER-2 did a series of vertical profiles as it first flew west over tropical storm Ingrid and then north to Houston. The DC-8 performed a regional chemistry survey. It proceeded up the Houston ship channel, sampling urban pollution and then proceeded to the coast of Northwest Florida, where terpene concentrations of 1 ppb and isoprene of 2 ppb were observed. The DC-8 then flew downwind of Atlanta, but probably did not penetrate the main plume from the city, though some urban emissions were detected. After reaching Kentucky, the aircraft turned southwest and flew down the polluted Ohio River Valley. Next, the DC-8 sampled the plumes from seven different agricultural fires, observing rapid smoke evolution. Near Houston the DC-8 profiled the upper troposphere hoping to catch blowoff from a pair of hurricanes straddling Mexico. The Learjet flew a CloudSat/CALIPSO overpass to sample anvil cirrus.

4.3.19. The 17 September 2013 Flight

The Learjet made a flight on this day as illustrated in Figure 37. The goal of this flight was to sample cirrus over the Gulf of Mexico during a MISR overpass.

4.3.20. The 18 September 2013 Flight

On this date, all three aircraft were flown as shown in Figure 38. The DC-8 first profiled the marine boundary layer in the vicinity of a number of offshore oil wells. Only limited emissions were observed, though the DC-8 flew at 500 ft above the surface. The ER-2 flew above thin cirrus in this region. All aircraft rendezvoused in a region with marine convection. The Learjet and the DC-8 penetrated the clouds at several levels, and the DC-8 profiled them with radar, while the ER-2 flew above the convective clouds making remote observations of cirrus. The three aircraft then moved to Southern Texas, targeting convective storms forecast to develop over major oil and gas extraction activities in the Eagle Ford Shale. En route, the ER-2 performed a vertical profile of the UTLS. Once over Texas the Learjet and DC-8 sampled convective clouds, while the ER-2 flew racetracks overhead to view the clouds remotely. Tracers indicating emissions from drilling and/or production of oil and gas were observed in the cloud tops between 33 and 37 kft. The DC-8 subsequently characterized these emissions flying in the boundary layer at 1000 ft. On its return to Houston, the DC-8 did a run with the DIAL lidar to support DISCOVER-AQ, then made four passes at progressively closer range (younger age) through the plume from the Houston ship channel, with the goal of assessing the relative importance of photochemical production versus direct release as sources of HCHO in this major petrochemical industrial region. The ER-2 flew several coordinated legs with the DC-8 over Houston and several AERONET sites located there. The ER-2 made a spiral descent over Ellington to obtain a vertical profile.

4.3.21. The 21 September 2013 Flight

The DC-8 flew on this day as shown in Figure 39. The DC-8 sampled a long cold front extending from Houston, north into the Northeast U.S. The aircraft did a series of legs at ascending altitudes over the Carolinas. Concentrations of tracers were not obviously enhanced except near one point where the APR2 radar noted a convective cell. The DC-8 then proceeded westward and encountered what appeared to be stratospherically influenced air over western Tennessee. The DC-8 descended into the boundary layer over the Ozarks. Isoprene and its products were observed, as was elevated NO_x. The Sun sets during this run so that nighttime isoprene chemistry was observed under a variety of NO_x concentrations.

4.3.22. The 22 September 2013 Flight

The ER-2 and the Learjet made a joint flight on this day as illustrated in Figure 40. The ER-2 flew several racetracks over marine stratus just south of Houston in conjunction with the Learjet. At the conclusion of this flight, the Learjet departed for home. The ER-2 continued to fly over cirrus associated with a cold front and made a vertical profile of the UTLS. It then flew over several AERONET sites located in Houston.

4.3.23. The 23 September 2013 Flight

On the final mission of the SEAC^{4}RS project, the DC-8 and the ER-2 flew independent flight profiles as illustrated in Figure 41. The ER-2 flew north along a CALIPSO/MLS Aura satellite track performing several vertical profiles to characterize the lower stratosphere. Along the way it flew over an MCC. On the south bound leg the aircraft

flew over the Bozeman optical supersite, where the aerosol optical thickness was quite low, to obtain data for the Air MSPI polarimeter. It then overflew the Railroad Valley, Nevada, AERONET site where optical thicknesses were also low. On the return to Palmdale the ER-2 made a slow descent to support the TCCON site. The DC-8 began its return flight with several passes over the Houston ship channel to characterize the local emissions. It then proceeded to the Ozarks to investigate isoprene emissions with cooler temperatures. Five agricultural fires were sampled in the Mississippi Valley, three of them multiple times. The transit to the west encountered what appeared to be stratospheric air in the UTLS and possibly aged marine air. Starting near the border between Arizona and California the aircraft did a boundary layer air chemistry run over Salton Sea, along Highway 10 and then along the north side of the Los Angeles basin. This run was nearly identical to a route flown on the last DC-8 test flight (5 August), but it was in the reverse direction and made later in the day. The DC-8 then did a missed approach at Edwards Air Force Base to complete the TCCON vertical profile from the ER-2 flight level near 65 kft to 100 ft above ground level.

5. Summary of SEAC^{4}RS Implementation and Some Initial Results

As summarized in Table 3, SEAC^{4}RS made many research flights that addressed each of the mission questions listed in Tables 1 and 2. SEAC^{4}RS was fortunate to have good weather, and no significant aircraft maintenance issues, which allowed 57 research flights. SEAC^{4}RS was also fortunate that a great variety of scientifically valuable targets were present within range of the aircraft. The purpose of this paper is to provide an overview of the goals of SEAC^{4}RS, an outline of the flights that were made to address these goals, and a map connecting the goals with the specific flights. This information should be useful to those who would like to use the SEAC^{4}RS data set in their research. The SEAC^{4}RS data set is now in the public domain and can be accessed at http://www-air.larc.nasa.gov/cgi-bin/ArcView/seac4rs. As outlined in Tables 1 and 2, a major goal of SEAC^{4}RS was to explore pollutant emissions. While flights were made across a wide expanse of the U.S. and the Gulf of Mexico, most flights were made in the Southeastern U.S. This region is of interest because declining emissions, particularly of SO_2 and NO_x (Figure 3) suggest that anthropogenic pollution has lessened to the extent that organic gases and aerosols now play a larger role than in past decades and that the atmospheric chemical pathways have changed.

Regional aerosol optical thickness and formaldehyde concentrations fell significantly between August and October of 2013 as temperatures cooled and organic emissions fell (Figures 4 and 5). While satellite retrieved optical thicknesses over the U.S. are not available prior to about 2002, visibility studies suggest that U.S. summertime aerosol optical thicknesses were highest in the Southeast prior to 1995 [e.g., *Schichtel et al.*, 2001], though year-to-year variability occurs due to the fluctuating abundance of Western wildfires. However, in August 2013, the optical thicknesses in the Northwestern U.S. and the plains states rivaled those in the Southeast, largely due to the numerous wildfires in the Northwest (Figure 4).

Several papers have been published using SEAC^{4}RS data to explore aerosol properties over the Southeastern U.S. *Wagner et al.* [2015] find that, contrary to previous theories, there was not a locally generated layer of enhanced organic aerosol aloft that had been suggested to explain the high summertime optical thickness over the Southeast. *Kim et al.* [2015] use SEAC^{4}RS data to show that the difference in seasonality between AOT, and surface aerosol concentrations mainly reflects seasonal differences in boundary layer depth. *Brock et al.* [2015a, 2015b] examined the sensitivity of AOT to humidity, and a variety of parameters such as boundary layer thickness, refractive index, and particle size. They also derived relationships between the hygroscopicity parameter and the extinction. *Schwartz et al.* [2014] used DC3 and SEAC^{4}RS data to develop an SP-2 instrument to measure the effects of humidification on particles containing black carbon. *Dolgos and Martins* [2014] describe a polarized imaging nephelometer that was used to measure the scattering phase function for aerosols.

Liao et al. [2015] investigated the abundances and formation of two types of organosulfates using data from DC3 and SEAC^{4}RS. They found these two compounds each comprise about 1% of the aerosol mass. Their formation was found to depend not only on the organic gas phase precursors but also on the emissions of sulfur dioxide, since aerosol acidity was important to the chemistry. *Marais et al.* [2015] develop an aqueous phase mechanism for isoprene SOA formation and also show strong coupling with SO_2 emissions through aerosol acidity. The composition of SOA is a complex and vexing issue. *Hu et al.* [2015] review a variety of data sets to investigate the amount of SOA formed from isoprene epoxydiols (IEPOX), which are an oxidation product of isoprene primarily under low NO_x conditions. *Hu et al.* [2015] find that IEPOX-SOA is often an important

fraction of all organic aerosol present in regions strongly influenced by isoprene emissions under low NO_x conditions and that $C_5H_6O^+$ is a good indicator for IEPOX-SOA. *Yu et al.* [2016] investigate the importance of grid resolution to properly modeling air chemistry in a region in which NO_x concentrations vary rapidly with distance.

The short lifetimes of the VOCs allowed for measurements of vertical flux to be made in some cases [*Wolfe et al.*, 2015] and for studying the evolution of aerosols as they were produced from the VOCs. These were the first eddy correlation flux experiments ever done with the DC-8.

Nitrogen oxides are an important element of atmospheric chemistry. SEAC^{4}RS was able to observe chemical processing over a wide range of NO_x abundances to explore the dependence of the chemistry on NO_x. *Teng et al.* [2015] report branching ratios for speciated hydroxy nitrates resulting from the oxidation of C_2 to C_8 monoalkenes. *Nault et al.* [2015] report the first measurements of methyl peroxy nitrate, which could be important for photochemistry at low temperatures in the upper troposphere.

Another major goal of SEAC^{4}RS was to explore the properties of smoke plumes emitted by a variety of types of fires. SEAC^{4}RS sampled smoke from many agricultural fires in the Southeast, as well as from numerous wildfires in the Western U.S. (Figure 6). Notably, the DC-8 was able to follow the smoke plume from the Rim Fire in California from its source near Yosemite Valley to Central Canada, possibly the longest transect of smoke ever made, offering an opportunity to study the evolution of smoke over several days since the time of emission. The Rim Fire burned the third largest area in California fire history. *Peterson et al.* [2015] and *Yates et al.* [2016] discuss many details of the Rim Fire evolution and plume composition.

One important issue for fires is to accurately determine the amount of emissions. *Saide et al.* [2015] found that standard methods for estimating total emissions require substantial modifications for extreme events such as the Rim Fire, particularly at night. Another important issue is determining the properties of brown carbon in smoke. Brown carbon is a mix of organic compounds containing many non-C atoms unlike black carbon, which is composed of pure C. It has been suggested that the UV absorption due to the large amounts of brown carbon emitted by fires has an important effect on atmospheric radiation [*Feng et al.*, 2013]. *Forrister et al.* [2015] show that in the Rim Fire most of the brown carbon light absorption decayed with a lifetime of 9–15 h. Some aerosol light absorption did persist. If this is the typical outcome for BB plumes, then brown carbon may be less important for climate than previously thought. Other smoke properties were determined by *Forrister et al.* [2015]. For example, they found that the black carbon was coated with a layer of material about 100 nm thick and that this coating did not change significantly during transport times exceeding 30 h. Fast formation of PAN and ozone and high emissions of sulfur and chlorine were observed for agricultural fires. Wildfires and agricultural fires are both major fire types that were little studied previously and were both sampled in great detail during SEAC^{4}RS. Both fire types are also expected to occur more frequently in the future due to climate change and increased food production [*Yue et al.*, 2015; *Tilman et al.*, 2001].

Existing data assimilation approaches for estimating smoke production were tested thoroughly and new satellite products, such as smoke over cloud AOT, were developed for future assimilation approaches. *Wu et al.* [2015] use SEAC^{4}RS data to explore the retrieval accuracies of aerosol properties over land from multiangle polarimetric measurments. *McHardy et al.* [2015] used ground-based SEAC^{4}RS instruments to develop techniques to measure nighttime aerosol optical thickness from VIIRS satellite data.

SEACIONS balloon observations in New Mexico between 8 and 14 August showed layers of low ozone and low humidity in the upper troposphere. The ozone in these layers was 1–2 standard deviations below the mean. The low ozone and low humidity layers were traced back to deep convection associated with Hurricane Henriette in the eastern/central tropical Pacific by *Minschwaner et al.* [2015].

These advances, especially in combination, will improve present and future atmospheric modeling of air quality, visibility, climate, and chemistry.

Acknowledgments
SEAC^{4}RS was organized and funded by the NASA Earth Science Program and the Naval Research Laboratory. We thank the aircraft managers, engineers, and ground crews of all the aircraft that participated in SEAC^{4}RS. We particularly thank the pilots of the ER-2 Tim Williams, Denis Steele, Dan Neely, and Stuart Broce; mobile pilot Jan Nystrom; and the DC-8 pilots Frank Batteas, Wayne Ringelberg, Manny Puerta, Denis Steele, Troy Asher, Nils Larson, and Bill Brockett. The DC-8 navigators, Carl Magnusson, Alan Rabb, Keith Schilawski, Ben Williams, Jeff Wilson, and Jeff Texcell were essential to flight planning and to helping adjust flight patterns in real time. NASA's Armstrong Flight Research Center Airborne Science Directorate provided excellent support for the aircraft. We thank Bruce Tagg, the Airborne Science Program manager; ER-2 aircraft mission managers, Tim Moes and Chris Miller; the DC-8 mission manager, Frank Cutler, as well as Rick Shetter. The NASA Ames Earth Science Project Office made tremendous contributions to the operations and overall success of SEAC^{4}RS. Our special thanks go to Kent Shiffer, Jhony Zavaleta, Mike Craig, David Jordan, Sue Tolley, Quincy Allison, Dan Chirica, Erin Czech, Erin Justice, and Katja Drdla. We are grateful for the support of the NASA Langley Clouds Group, especially Rabi Palikonda, Louis Nguyen, Kris Bedka, Bill Smith, Jr., Kirk Ayers, Chris Yost, Doug Spangenberg, Michele Nordeen, Dave Duda, Robyn Boeke, Thad Chee, and Ben Scarino. We appreciated Kathy Thompson for her dedication and effort throughout the planning and postmission analysis of SEAC4RS. The airport personnel at NASA's Johnson spaceflight center and Ellington Field were very helpful to the mission. We especially thank Dick Clark, Chief of the Aircraft Operations Division; Gary Ash, Chief of Aircraft Maintenance; Arne Aamodt and Kevin Lasenski from the Aircraft Operations Division; Noreen McLeroy for IT support; Lisa Buswell, Administrative Officer; Rose Garder, International Visits Coordinator; and, Frank Newman for laboratory and building support in Building 994. Jim Crawford, at NASA's Langley Research Center, played a key role in planning the SEAC^{4}RS field mission. The SEAC^{4}RS data are now in the public domain and can be accessed at http://www-air.larc.nasa.gov/cgi-bin/ArcView/seac4rs. Alternatively one can locate the data at www.doi.org using doi:10.5067/Aircraft/SEAC4RS/Aerosol-TraceGas-Cloud. O. B. Toon was supported by NASA awards NNX12AC64G and NNX14AR56G.

References

Akagi, S. K., R. J. Yokelson, C. Wiedinmyer, M. J. Alvarado, J. S. Reid, T. Karl, J. D. Crounse, and P. O. Wennberg (2011), Emission factors for open and domestic biomass burning for use in atmospheric models, *Atmos. Chem. Phys.*, *11*, 4039–4072, doi:10.5194/acp-11-4039-2011.

Anderson, J. G., D. M. Wilmouth, J. B. Smith, and D. S. Sayers (2012), UV dosage levels in summer: Increased risk of ozone loss from convectively injected water vapor, *Science*, *337*, 835–839, doi:10.1126/science.1222978.

Ashley, W. S., T. L. Mote, P. G. Dixon, S. L. Trotter, E. J. Powell, J. D. Durkee, and A. J. Grundstein (2003), Distribution of mesoscale convective complex rainfall in the United States, *Mon. Weather Rev.*, *131*, 3003–3017.

Barkley, M. P., et al. (2013), Top-down isoprene emissions over tropical South America inferred from SCIAMACHY and OMI formaldehyde columns, *J. Geophys. Res. Atmos.*, *118*, 6849–6868, doi:10.1002/jgrd.50552.

Barth, M. C., et al. (2014), The deep convective clouds and chemistry (DC3) field campaign, *Bull. Am. Meteorol. Soc.*, *96*, 1281–1309, doi:10.1175/BAMS-D-13-00290.1.

Bedka, K. M., J. Brunner, R. Dworak, W. Feltz, J. Otkin, and T. Greenwald (2010), Objective satellite-based overshooting top detection using infrared window channel brightness temperature gradients, *J. Appl. Meteorol. Climatol.*, *49*, 181–202.

Brock, C. A., et al. (2015a), Aerosol optical properties in the southeastern United States in summer—Part 1: Hygroscopic growth, *Atmos. Chem. Phys. Discuss.*, *15*, 25,695–25,738, doi:10.5194/acpd-15-25695-2015.

Brock, C. A., et al. (2015b), Aerosol optical properties in the southeastern United States in summer—Part 2: Sensitivity of aerosol optical depth to relative humidity and aerosol parameters, *Atmos. Chem. Phys. Discuss.*, *15*, 31,471–31,499, doi:10.5194/acpd-15-31471-2015.

Chance, K., P. Palmer, R. J. D. Spurr, R. V. Martin, T. Kurosu, and D. J. Jacob (2000), Satellite observations of formaldehyde over North America from GOME, *Geophys. Res. Lett.*, *27*, 3461–3464, doi:10.1029/2000GL011857.

de Laat, A. T. J., D. C. Stein Zweers, R. Boers, and O. N. E. Tuinder (2012), A solar escalator: Observational evidence of the self-lifting of smoke and aerosols by absorption of solar radiation in the February 2009 Australian Black Saturday plume, *J. Geophys. Res.*, *117*, D04204, doi:10.1029/2011JD017016.

Dessler, A. E., and S. C. Sherwood (2003), A model of HDO in the tropical tropopause layer, *Atmos. Chem. Phys.*, *3*, 2173–2181, doi:10.5194/acp-3-2173-2003.

Dessler, A. E., T. F. Hanisco, and S. Fueglistaler (2007), Effects of convective ice lofting on H_2O and HDO in the tropical tropopause layer, *J. Geophys. Res.*, *112*, D18309, doi:10.1029/2007JD008609.

Dolgos, G., and J. V. Martins (2014), Polarized imaging nephelometer for in situ airborne measurements of aerosol light scattering, *Opt. Express*, *22*, 21,972–21,990.

Environmental Protection Agency (EPA) (2011), Integrated science assessment for ozone and related photochemical oxidants, EPA/600/R-10/076A.

Environmental Protection Agency (EPA) (2014), 1970–2013 Average annual emissions, all criteria pollutants in MS Excel, Feb 2014. [Available at http://www.epa.gov/ttn/chief/trends/index.html, Feb 20, 2015.]

Feng, Y., V. Ramanathan, and V. R. Kotamarthi (2013), Brown carbon: A significant atmospheric absorber of solar radiation?, *Atmos. Chem. Phys.*, *13*, 8607–8621, doi:10.5194/acp-13-8607-2013.

Ford, B., and C. L. Heald (2013), Aerosol loading in the Southeastern United States: Reconciling surface and satellite observations, *Atmos. Chem. Phys.*, *13*, 9269–9283, doi:10.5194/acp-13-9269-2013.

Forrister, H., et al. (2015), Evolution of brown carbon in wildfire plumes, *Geophys. Res. Lett.*, *42*, 4623–4630, doi:10.1002/2015GL063897.

Fromm, M. D., and R. Servranckx (2003), Transport of forest fire smoke above the tropopause by supercell convection, *Geophys. Res. Lett.*, *30*(10), 1542, doi:10.1029/2002GL016820.

Fromm, M. D., J. Alfred, K. Hoppel, J. Hornstein, R. Bevilacqua, R. E. Shettle, R. Servranckx, Z. Li, and B. Stocks (2000), Observations of boreal forest fire smoke in the stratosphere by POAM III, SAGE II, and lidar in 1988, *Geophys. Res. Lett.*, *27*, 1407–1410, doi:10.1029/1999GL011200.

Goldstein, A. H., C. D. Koven, C. L. Heald, and I. Y. Fung (2009), Biogenic carbon and anthropogenic pollutants combine to form a cooling haze over the southeastern United States, *Proc. Natl. Acad. Sci. U.S.A.*, *106*, 8835–8840, doi:10.1073/pnas.0904128106.

Guenther, A. B., X. Jiang, C. L. Heald, T. Sakulyanontvittaya, T. Duhl, L. K. Emmons, and X. Wang (2012), The Model of Emissions of Gases and Aerosols from Nature version 2.1 (MEGAN2.1): An extended and updated framework for modeling biogenic emissions, *Geosci. Model Dev.*, *5*, 1471–1492, doi:10.5194/gmd-5-1471-2012.

Hanisco, T. F., et al. (2007), Observations of deep convective influence on stratospheric water vapor and its isotopic composition, *Geophys. Res. Lett*, *34*, L04814, doi:10.1029/2006GL027899.

Hidy, G. M., C. L. Blanchard, K. Baumann, E. Edgerton, S. Tanenbaum, S. Shaw, E. Knipping, I. Tombach, J. Jansen, and J. Walters (2014), Chemical climatology of the southeastern United States, 1999–2013, *Atmos. Chem. Phys.*, *14*, 11,893–11,914.

Holton, J. R., et al. (1995), Stratosphere-troposphere exchange, *Rev. Geophys.*, *33*, 403–439, doi:10.1029/95RG02097.

Homeyer, C. R., et al. (2014), Convective transport of water vapor into the lower stratosphere observed during double-tropopause events, *J. Geophys. Res. Atmos.*, *119*, 10,941–10,958, doi:10.1002/2014JD021485.

Hoor, P., H. Fischer, L. Lange, J. Lelieveld, and D. Brunner (2002), Seasonal variations of a mixing layer in the lowermost stratosphere as identified by the CO-O-3 correlation from in situ measurements, *J. Geophys. Res.*, *107*(D5), 4044 doi:10.1029/2000JD000289.

Hu, W. W., et al. (2015), Characterization of a real-time tracer for Isoprene Epoxydiols-derived Secondary Organic Aerosol (IEPOX-SOA) from aerosol mass spectrometer measurements, *Atmos. Chem. Phys.*, *15*, 11,807–11,833, doi:10.5194/acp-15-11807-2015.

Jensen, E. J., D. Starr, and O. B. Toon (2004), Mission investigates tropical cirrus clouds, *Eos Trans. AGU*, *85*, 45–50.

Jost, H. J., et al. (2004), In-situ observations of mid-latitude forest fire plumes deep in the stratosphere, *Geophys. Res. Lett.*, *31*, L11101, doi:10.1020/2003GL019253.

Khaiyer, M. M., M. L. Nordeen, R. Palikonda, Y. Yi, P. Minnis, and D. R. Doelling (2009), Validation of improved broadband shortwave and longwave fluxes derived from GOES, Proc. 16th AMS Conf. Sat. Meteorol. & Oceanog., Phoenix, Ariz., 12-15 Jan.

Kim, P. S., et al. (2015), Sources, seasonality, and trends of Southeast U.S. aerosol: An integrated analysis of surface, aircraft, and satellite observations with the GEOS-Chem model, *Atmos. Chem. Phys.*, *15*, 10,411–10,433, doi:10.5194/acp-15-10411-2015.

Liao, J., et al. (2015), Airborne measurements of organosulfates over the continental U.S., *J. Geophys. Res. Atmos.*, *120*, 2990–3005, doi:10.1002/2014JD022378.

Marais, E. A., et al. (2012), Isoprene emissions in Africa inferred from OMI observations of formaldehyde columns, *Atmos. Chem. Phys.*, *12*, 6219–6235.

Marais, E. A., D. J. Jacob, A. Guenther, K. Chance, T. P. Kurosu, J. G. Murphy, C. E. Reeves, and H. Pye (2014), Improved model of isoprene emissions in Africa using OMI satellite observations of formaldehyde: Implications for oxidants and particulate matter, *Atmos. Chem. Phys.*, *14*, 7693–7703.

Marais, E. A., et al. (2015), Aqueous-phase mechanism for secondary organic aerosol formation from isoprene: Application to the Southeast United States and co-benefit of SO_2 emission controls, *Atmos. Chem. Phys.*, *15*, 32,005–32,047, doi:10.5194/acpd-15-32005-2015.

McHardy, T. M., J. Zhang, J. S. Reid, S. D. Miller, E. J. Hyer, and R. E. Kuehn (2015), An improved method for retrieving nighttime aerosol optical thickness from VIIRS Day/Night Band, *Atmos. Meas. Tech. Discuss.*, *8*, 5147–5178.

Millet, D. B., et al. (2006), Formaldehyde distribution over North America: Implications for satellite retrievals of formaldehyde columns and isoprene emission, *J. Geophys. Res.*, *111*, D24S02, doi:10.1029/2005JD006853.

Millet, D. B., D. J. Jacob, K. F. Boersma, T. Fu, T. P. Kurosu, K. Chance, C. L. Heald, and A. Guenther (2008), Spatial distribution of isoprene emissions from North America derived from formaldehyde column measurements by the OMI satellite sensor, *J. Geophys. Res.*, *113*, D02307, doi:10.1029/2007JD008950.

Minnis, P., and W. L. Smith Jr. (1998), Cloud and radiative fields derived from GOES-8 during SUCCESS and the ARM-UAV spring 1996 flight series, *Geophys. Res. Lett.*, *25*, 1113–1116, doi:10.1029/98GL00301.

Minnis, P., S. Sun-Mack, D. F. Young, P. W. Heck, D. P. Garber, et al. (2011), CERES Edition-2 cloud property retrievals using TRMM VIRS and Terra and Aqua MODIS data, Part I: Algorithms, *IEEE Trans. Geosci. Remote Sens.*, *49*, 4374–4400.

Minschwaner, K. R., et al. (2015), Signature of a tropical Pacific cyclone in the composition of the upper troposphere over Socorro, NM, *Geophys. Res. Lett.*, *42*, 9530–9537, doi:10.1002/2015GL065824.

Nault, B. A., C. Garland, S. E. Pusede, P. J. Wooldridge, K. Ullmann, S. R. Hall, and R. C. Cohen (2015), Measurements of $CH_3O_2NO_2$ in the upper troposphere, *Atmos. Meas. Tech.*, *8*, 987–997.

Palmer, P. I., D. J. Jacob, A. M. Fiore, R. V. Martin, K. Chance, and T. Kurosu (2003), Mapping isoprene emissions over North America using formaldehyde column observations from space, *J. Geophys. Res.*, *108*(D6), 4180, doi:10.1029/2002JD002153.

Palmer, P. I., et al. (2006), Quantifying the seasonal and interannual variability of North American isoprene emissions using satellite observations of formaldehyde column, *J. Geophys. Res.*, *111*, D12315, doi:10.1029/2005JD006689.

Pan, L. L., W. J. Randel, B. L. Gary, M. J. Mahoney, and E. J. Hintsa (2004), Definitions and sharpness of the extratropical tropopause: A trace gas perspective, *J. Geophys. Res.*, *109*, D23103, doi:10.1029/2004JD004982.

Pan, L. L., et al. (2007), Chemical behavior of the tropopause observed during the Stratosphere-Troposphere Analyses of Regional Transport (START) experiment, *J. Geophys. Res.*, *112*, D18110, doi:10.1029/2007JD008645.

Park, M., W. J. Randel, A. Gettelman, S. Massie, and J. Jiang (2007), Transport above the Asian summer monsoon anticyclone inferred from Aura MLS tracers, *J. Geophys. Res.*, *112*, D16309, doi:10.1029/2006JD008294.

Peterson, D. A., E. J. Hyer, J. R. Campbell, M. D. Fromm, J. W. Hair, C. F. Butler, and M. A. Fenn (2015), The 2013 Rim fire: Implications for predicting extreme fire spread, pyroconvection, and smoke emissions, *Bull. Am. Meteorol. Soc.*, *96*, 229–247, doi:10.1175/BAMS-D-14-00060.1.

Randel, W. J., M. Park, L. Emmons, D. Kinnison, P. Bernath, K. Walker, C. Boone, and H. Pumphrey (2010), Asian monsoon transport of pollution to the stratosphere, *Science*, *328*, 611–613, doi:10.1126/science.1182274.

Randel, W. J., E. Moyer, M. Park, E. Jensen, P. Bernath, K. Walker, and C. Boone (2012), Global variations of HDO and HDO/H_2O ratios in the upper troposphere and lower stratosphere derived from ACE-FTS satellite measurements, *J. Geophys. Res.*, *117*, D06303, doi:10.1029/2011JD016632.

Read, W. G., et al. (2007), Aura Microwave Limb Sounder upper tropospheric and lower stratospheric H_2O and relative humidity with respect to ice validation, *J. Geophys. Res.*, *112*, D24S35, doi:10.1029/2007JD008752.

Saide, P. E., et al. (2015), Revealing important nocturnal and day-to-day variations in fire smoke emissions through a multiplatform inversion, *Geophys. Res. Lett.*, *42*, doi:10.1002/2015GL063737.

Schichtel, B. A., R. B. Husar, S. R. Falke, and W. E. Wilson (2001), Haze trends over the United States, 1980–1995, *Atmos. Environ.*, *35*, 5205–5210.

Schoeberl, M. R., A. E. Dessler, and T. Wang (2013), Modeling upper tropospheric and lower stratospheric water vapor anomalies, *Atmos. Phys. Chem.*, *13*, 7783–7793.

Schwartz, J. P., A. E. Perring, M. Z. Markovic, R. S. Gao, S. Ohata, J. Langridge, D. Law, R. McLaughlin, and D. W. Fahey (2014), Technique and theoretical approach for quantifying the hygroscopicity of black-carbon-containing aerosol using a single particle soot photometer, *J. Aerosol Sci.*, *81*, 110–126.

Schwartz, M. J., W. G. Read, M. L. Santee, N. J. Livesey, L. Froidevaux, A. Lambert, and G. L. Manney (2013), Convectively injected water vapor in the North American summer lowermost stratosphere, *Geophys. Res. Lett.*, *40*, 2316–2321, doi:10.1002/grl.50421.

Solomon, S., K. H. Rosenlof, R. W. Portmann, J. S. Daniel, S. M. Davis, T. J. Sanford, and G.-K. Plattner (2010), Contributions of stratospheric water vapor to decadal changes in the rate of global warming, *Science*, *327*, 1219–1223, doi:10.1126/science.1182488.

Teng, A. P., J. D. Crounse, L. Lee, J. M. St. Clair, R. C. Cohen, and P. O. Wennberg (2015), Hydroxy nitrate production in the OH-initiated oxidation of alkenes, *Atmos. Chem. Phys.*, *15*, 4297–4316, doi:10.5194/acp-15-4297-2015.

Thomason, L. W., and J.-P. Vernier (2013), Improved SAGE II cloud/aerosol categorization and observations of the Asian tropopause aerosol layer: 1989–2005, *Atmos. Chem. Phys.*, *13*, 4605–4616, doi:10.5194/acp-13-4605-2013.

Tilman, D., J. Fargione, B. Wolff, C. D'Antonio, A. Dobson, R. Howarth, D. Schindler, W. H. Schlesinger, D. Simberloff, and D. Swackhamer (2001), Forecasting agriculturally driven global environmental change, *Science*, *292*, 281–284, doi:10.1126/science.1057544.

Toon, O. B., et al. (2010), Planning, implementation, and first results of the Tropical Composition, Cloud and Climate Coupling Experiment (TC4), *J. Geophys. Res.*, *115*, D00J04, doi:10.1029/2009JD013073.

Vernier, J.-P., L. W. Thomason, and J. Kar (2011), CALIPSO detection of an Asian tropopause aerosol layer, *Geophys. Res. Lett.*, *38*, L07804, doi:10.1029/2010GL046614.

Vernier, J.-P., T. D. Fairlie, M. Natarajan, F. G. Wienhold, J. Bian, B. G. Martinsson, S. Crumeyrolle, L. W. Thomason, *and* K. Bedka (2015), Increase in upper tropospheric and lower stratospheric aerosol levels and its potential connection with Asian pollution, *J. Geophys. Res. Atmos.*, *120*, 1608–1619, doi:10.1002/2014JD022372.

Wagner, N. L., et al. (2015), In situ vertical profiles of aerosol extinction, mass, and composition over the southeast United States during SENEX and SEAC^{4}RS: Observations of a modest aerosol enhancement aloft, *Atmos. Chem. Phys.*, *15*, 7085–7102, doi:10.5194/acp-15-7085-2015.

Wolfe, G. M., et al. (2015), Quantifying sources and sinks of reactive gases in the lower atmosphere using airborne flux observations, *Geophys. Res. Lett.*, *42*, 8231–8240, doi:10.1002/2015GL065839.

Wu, L., O. Hasekamp, B. van Diedenhoven, and B. Cairns (2015), Aerosol retrieval from multiangle, multispectral photopolarimetric measurements: Importance of spectral range and angular resolution, *Atmos. Means. Tech.*, *8*, 2625–2638.

Yates, E. L., et al. (2016), Airborne measurements and emission estimates of greenhouse gases and other trace constituents from the 2013 California Yosemite Rim wildfire, *Atmos. Environ.*, *127*, 293–302.

Yu, K., et al. (2016), Sensitivity to grid resolution in the ability of a chemical transport model to simulate observed oxidant chemistry under high-isoprene conditions, *Atmos. Chem. Phys. Discuss.*, doi:10.5194/acp-2015-980.

Yu, P., O. B. Toon, R. R. Neely, B. G. Martinsson, and B. G. Brenninkmeijer (2015), Composition and physical properties of the Asian tropopause aerosol layer and the North American tropopause aerosol layer, *Geophys. Res. Lett.*, *42*, 2540–2546, doi:10.1002/2015GL063181.

Yue, X., L. J. Mickley, J. A. Logan, R. C. Hudman, M. V. Martin, and R. M. Yantosca (2015), Impact of 2050 climate change on North American wildfire: Consequences for ozone air quality, *Atmos. Chem. Phys.*, *15*, 10,033–10,055, doi:10.5194/acp-15-10033-2015.

Zhu, L., D. J. Jacob, L. J. Mickley, E. A. Marais, D. S. Cohan, Y. Yoshida, B. N. Duncan, G. González Aba, and K. V. Chance (2014), Anthropogenic emissions of highly reactive volatile organic compounds in eastern Texas inferred from oversampling of satellite (OMI) measurements of HCHO columns, *Environ. Res. Lett.*, *9*, 11404, doi:10.1088/1748-9326/9/11/114004.